Hamiltonian formulation of non-Abelian gauge fields and nonrelativistic bound states

Frank L. Feinberg

Center for Theoretical Physics, Laboratory for Nuclear Science and Department of Physics, Massachusetts Institute of Technology, Cambridge, Massachusetts 02139

(Received 19 December 1977)

For fermions minimally coupled to non-Abelian gauge fields, first-order quantization in the radiation gauge is presented in which the validity of naive Ward identities simplifies the renormalization procedure. Then, successive Foldy-Wouthuysen transformations are used to determine the nonrelativistic Hamiltonian operator as well as its first relativistic correction. This operator expansion is verified to all orders of perturbation theory by an extension of the Appelquist-Carazzone decoupling theorem. Next, the Hamiltonian, which provides a systematic starting point for any nonrelativistic calculation, is used to cast the fermion-antifermion nonrelativistic bound-state kernel into a simple and compact form which is spin independent and serves as the basis of a perturbative analysis. Through two loops, calculation of the kernel reveals that a mass-independent static potential exists in the nonrelativistic limit only for singlet states of the gauge group. Higher-loop corrections, three-fermion bound states, and nonperturbative methods are also discussed.

I. INTRODUCTION

Phenomenological analyses[1] of the J/ψ family of particles have indicated many unique features of this system. One such feature is the good agreement of nonrelativistic potential models with both the mass spectrum of the particles and with the electromagnetic transitions of the various states. A natural inference, therefore, is that this physical system exhibits the nonrelativistic limit of the strong interactions. Furthermore, this kinematic region may possess sufficient dynamical simplifications to make mathematical analysis more tractable. In this paper, an elaboration and continuation of a previous work,[2] a systematic formalism is developed for describing hadronic systems in the nonrelativistic limit as well as for obtaining relativistic corrections. The dynamical model is that of one massive fermion minimally coupled to massless non-Abelian gauge fields, or quantum chromodynamics (QCD). Moreover, for nonrelativistic systems a clear physical interpretation is possible in the radiation or Coulomb gauge, as used in conventional treatments of the hydrogen atom. Also in the radiation gauge, use of the first-order canonical quantization eliminates unphysical ghosts.

In Sec. II a review of this quantization is presented with emphasis on the operator nature of the Coulomb interaction. The renormalization procedure, discussed in Sec. III, relies on Ward identities identical in form to the quantum-electrodynamics (QED) Ward identity, $Z_1 = Z_2$, and in addition facilitates nonrelativistic calculations. For describing nonrelativistic electrodynamical systems the unitary Foldy-Wouthuysen transformation provides a convenient representation for the free Dirac Hamiltonian[4] and also for systems of one or two fermions interacting with external electromagnetic fields.[5] This same type of transformation is also relevant here to provide the nonrelativistic reduction of the non-Abelian Hamiltonian. In Sec. IV three successive Foldy-Wouthuysen operator transformations are performed on the first-order radiation-gauge Hamiltonian to obtain its nonrelativistic limit and the first relativistic corrections to it. The physical interpretation of these correction terms is given by analogy with the corresponding QED corrections and phenomenological implications are discussed. The validity of the operator expansion is verified to all orders of perturbation theory in Sec. V.

As an explicit and relevant illustration of this formalism nonrelativistic fermion-antifermion bound states are studied in perturbation theory based on the Hamiltonian operator. The single Coulomb exchange gives the exact nonrelativistic potential in QED and bound states are found only for weakly coupled systems ($\alpha \sim v/c \ll 1$), but in the non-Abelian model, since the kernel is more complicated, the condition for threshold bound states is not necessarily that of small coupling. In the quark model, the J/ψ particle is a threshold quark-antiquark bound state of charmed quarks, heavy in the sense that their kinetic energy is small compared to their apparent mass. The nonrelativistic bound-state equation for fermion-antifermion bound states is discussed in Sec. VI and a simple and compact form of the nonrelativistic kernel is derived, spin independent to all orders of perturbation theory. In this kernel, the role of the fermions is that of spatially fixed external sources of Coulomb lines which then interact through the Yang-Mills interactions.

A detailed perturbative analysis of this kernel is presented in Sec. VII through sixth order. Sim-

ilar analyses have been done recently by Appelquist *et al.*,[6,7] Fischler and Susskind,[8] and related work has been done by Poggio.[9] If the fermions are sufficiently massive, then indeed the single Coulomb exchange will dominate the non-Abelian kernel with coupling constant $g(t)$. However, since the mass at which the single Coulomb exchange determines the potential is about 50 GeV (Refs. 1, 10), finite orders of perturbation theory cannot determine all physically important contributions to the kernel for presently known particles. However, general features may be apparent from low orders of the perturbation expansion. For example, at the two-loop level, the analysis in Sec. VII shows that the potential, a function of $g(t)$, has a well-defined static limit for gauge-group singlet states, whereas for nonsinglet states there is no static potential. This result indicates a possibly fundamental distinction between singlet and nonsinglet states, as is expected in confinement models, since it is a direct consequence of charge conservation. The same distinction occurs through two loops for three-fermion bound states, which are briefly discussed. However, in three loops there are apparent binding-energy dependences in the kernel, the significance of which has been considered by Appelquist *et al.*[7] A discussion of this energy dependence in the kernel, possible nonperturbative techniques, and the conclusion are presented in Sec. VIII.

II. FIRST-ORDER QUANTIZATION IN THE RADIATION GAUGE

For the model field theory of fermions minimally coupled to non-Abelian gauge fields, QCD, local gauge invariance requires isolation of the dynamical variables before quantization can be imposed. Even though manifest Lorentz invariance is lost, the radiation (or Coulomb) gauge condition determines a useful set of dynamical quantities, which are analogous to the QED radiation-gauge variables used for hydrogen-like systems. In addition, the physical picture in this gauge is improved by using a first-order formulation which eliminates the ghost states needed in second-order form. Moreover, this approach, used in the original quantization of the model by Schwinger,[11,12] is particularly relevant for nonrelativistic systems, as discussed in Sec. IV, although in this section the fully relativistic quantization is presented. Because this formulation is not used extensively, it is worthwhile to review it and to develop the perturbation theory rules. The Lagrangian density is given by

$$\mathcal{L}(x)=\tfrac{1}{4}F^a_{\mu\nu}F^{\mu\nu}_a-\tfrac{1}{2}F^a_{\mu\nu}(\partial^\mu A^\nu_a-\partial^\nu A^\mu_a+gf_{abc}A^\mu_bA^\nu_c)+\bar\psi(i\not\partial-gt^a\not A_a)\psi-m\bar\psi\psi\,, \tag{2.1}$$

where A^a_μ and $F^a_{\mu\nu}$ are the dynamical vector-meson coordinates, not all of which are independent. f_{abc} are the structure constants of the gauge group and t^a are the representation matrices of this group for the fermions. The above Lagrangian density gives the following Euler-Lagrange equations of motion:

$$F^{\mu\nu}_a=\partial^\mu A^\nu_a-\partial^\nu A^\mu_a+gf_{abc}A^\mu_bA^\nu_c\,, \tag{2.2a}$$

$$\partial_\mu F^{\mu\nu}_a+gf_{abc}A^b_\mu F^{\mu\nu}_c=\bar\psi\gamma^\nu gt^a\psi\,, \tag{2.2b}$$

$$(i\not\partial-gt^a\not A_a-m)\psi=0\,. \tag{2.2c}$$

The possible independent variables are A^a_i, F^a_{0i}, ψ, and $\psi^\dagger$ (Greek indices μ, ν,... run from 0 to 3; Roman indices $i,j,\ldots$ run from 1 to 3; Roman indices $a,b,\ldots$ are gauge-group indices). Since A^a_0 does not have a canonical momentum it must be a dependent variable and will be expressed in terms of independent quantities below. In addition, the time component of Eq. (2.2b) is a constraint equation,

$$(\delta_{ab}\partial_i+gf_{acb}A^c_i)F^{i0}_b=\psi^\dagger gt^a\psi\,, \tag{2.3}$$

which implies that not all of the A^a_i and F^a_{0i} are independent. To eliminate the ambiguity in defining the operators A^a_k the radiation-gauge condition is chosen:

$$\vec\nabla\cdot\vec A^a=0\,. \tag{2.4}$$

Also, division of F^a_{0i} into longitudinal and transverse parts isolates the Coulomb part of the interaction,

$$F^a_{0i}=F^{Ta}_{0i}+F^{La}_{0i}\,, \tag{2.5}$$

where $\vec\nabla\cdot\vec F^{Ta}_0=0$ and $\epsilon_{ijk}\partial_jF^{La}_{0i}=0$. The longitudinal part of F^a_{0i} can be expressed in terms of a scalar potential

$$F^{La}_{0i}\equiv-\partial_i\varphi^a \tag{2.6}$$

and the transverse part of F^a_{0i} is defined to be the electric field $\vec E^a$,

$$F^{Ta}_{0i}\equiv E^a_i\,. \tag{2.7}$$

In terms of these variables the dynamical operators are $\vec A^a,\psi$ (where $\vec\nabla\cdot\vec A^a=0$) and the canonically conjugate momenta $\vec E^a,\psi^\dagger$ (where $\vec\nabla\cdot\vec E^a=0$). The constraint equation, Eq. (2.3), now becomes

$$(\delta_{ab}\vec\nabla^2+gf_{acb}\vec A^c\cdot\vec\nabla)\varphi^b=gf_{acb}\vec A^c\cdot\vec E^b-\psi^\dagger gt^a\psi\,. \tag{2.8}$$

Equation (2.8) suggests the introduction of the following notation:

$$j^0_a(x)=-gf_{acb}\vec E^b\cdot\vec A^c+\psi^\dagger_gt^a\psi\,, \tag{2.9}$$

$$\mathfrak{D}^{ab}(x,y)=-(\vec\nabla^2\delta_{ab}+gf_{acb}\vec A_c\cdot\vec\nabla)^{-1}\,, \tag{2.10}$$

where $j^0_a(x)$ is the charge density of the non-Abelian theory and $\mathfrak{D}^{ab}(x,y)$ is the Green's func-

tion which determines $\phi^a(x)$ in terms of $j_a^0(x)$. In this paper it is assumed that this operator is well defined or, equivalently, that there are no ambiguities in defining the radiation gauge. This assumption, not true for large fields,[13,14] does not affect the perturbative analysis of this paper. Equation (2.10) is equivalent to

$$-(\vec{\nabla}_x^2\delta_{ab}+gf_{acb}\vec{A}_c\cdot\vec{\nabla}_x)\mathfrak{D}^{bd}(x,y)=\delta_{ad}\delta^3(\vec{x}-\vec{y})\,. \quad (2.11)$$

In terms of these functions the scalar potential, now an operator depending on $\vec{A}_a(x)$, is

$$\varphi^a(x)=\int d^3y\,\mathfrak{D}^{ab}(x,y)j_b^0(y)\,, \quad (2.12)$$

where $y^0=x^0$. Also, taking the divergence of Eq. (2.2a) for $\mu=0$ expresses A_0^a, the generalization of the Coulomb field, in terms of $\vec{A}^a$ and j_a^0:

$$A_a^0(x)=\int d^3y\,\mathfrak{D}^{ab}(x,y)\vec{\nabla}^2\varphi^b(y) \quad (2.13a)$$

$$=\int d^3y\,d^3z\,\mathfrak{D}^{ab}(x,y)\vec{\nabla}_y^2\mathfrak{D}^{bc}(y,z)j_c^0(z)\,. \quad (2.13b)$$

In all spatial integrals of the above type, the various time coordinates are equal.

In terms of the above variables, the Hamiltonian becomes

$$H=\int d^3x\left(\vec{E}_a\cdot\frac{\partial\vec{A}^a}{\partial t}+i\psi^\dagger\frac{\partial\psi}{\partial t}-\mathfrak{L}\right) \quad (2.14a)$$

$$=\int d^3x\,[\tfrac{1}{2}(\vec{E}^a\cdot\vec{E}_a+\vec{B}^a\cdot\vec{B}_a)+\psi^\dagger(-i\vec{\alpha}\cdot\vec{\nabla}+\beta m)\psi$$

$$-g\psi^\dagger\vec{\alpha}t^a\psi\cdot\vec{A}_a+\tfrac{1}{2}(\vec{\nabla}\varphi_a)\cdot(\vec{\nabla}\varphi^a)]\,, \quad (2.14b)$$

where $B_i^a=\frac{1}{2}\epsilon_{ijk}F_{jk}^a$. An additional term necessary for Lorentz covariance, found by Schwinger,[12] will not enter the perturbative calculations of Sec. VII and is omitted here. The last term is analogous to the Coulomb interaction in the Abelian theory and can be written in terms of the charge density $j_a^0(x)$ as

$$H_I^{\text{Coulomb}}=\int d^3x\,\tfrac{1}{2}(\vec{\nabla}\varphi_a)\cdot(\vec{\nabla}\varphi^a)$$

$$=\int d^3x\,d^3z\,d^3y\,[j_a^0(x)\mathfrak{D}_{ac}(x,z)\vec{\nabla}_z^2\mathfrak{D}_{cb}(z,y)j_0^b(y)]\,. \quad (2.15)$$

Note that $Q_a\equiv\int d^3x\,j_a^0(x)$ is the time-independent generator of the non-Abelian symmetry group. Also $\int d^3t\,\mathfrak{D}^{ac}(x,z)\vec{\nabla}_z^2\mathfrak{D}^{cb}(z,y)$ is the generalization of the QED Coulomb Green's function, so that Eq. (2.15) is the general form of the static non-Abelian longitudinal interaction with only the explicit form of $j_a^0(x)$ depending on the type of particles interacting with the gauge fields. In the nonrelativistic limit this part of the interaction is unchanged. Furthermore, each of the other terms in Eq. (2.14b) is directly analogous to the QED Hamiltonian.

The derivation of the perturbation theory rules from Eq. (2.14) is straightforward except for the Coulomb term. This term may be symbolically written as

$$-\tfrac{1}{2}\varphi_a\vec{\nabla}^2\varphi^a=-\frac{1}{2}\left[\left(\frac{1}{\vec{\nabla}^2+g\vec{A}\cdot\vec{\nabla}}\right)_{ab}j_b^0\right]\vec{\nabla}^2\left(\frac{1}{\vec{\nabla}^2+g\vec{A}\cdot\vec{\nabla}}\right)_{ac}j_c^0\,, \quad (2.16)$$

where $(\vec{A})_{ac}\equiv f_{acb}\vec{A}_b$ and the inverse operators, $\mathfrak{D}^{ab}$, are expanded as integral operators in a power series in g. From this expansion the perturbative rules for the Coulomb term are determined and the radiation-gauge perturbation-theory rules which result are given in Table I. It is important to realize that the use of the Coulomb force as an effective particle in Table I is introduced into the perturbation theory because it is a very useful technique for representing the spatially nonlocal static interactions of the longitudinal part of F_{0i}^a and A_a^0.

III. WARD IDENTITIES AND RENORMALIZATION

The appropriate choice of renormalization procedure is determined not only by the physical system under investigation but also by the ability to express most simply the requirements of gauge invariance. Here the renormalization scheme is motivated by the nonrelativistic character of the bound states studied in Secs. VI and VII, and by the existence of elegant and simple Ward identities derived below. Moreover, the perturbative calculations of Sec. VII verify these Ward identities through order g^6 for the vertex functions and propagators considered. In first-order form the Lagrangian density may be written as

$$\mathfrak{L}(x)=-\tfrac{1}{2}(\vec{E}_a^{\,2}+\vec{B}_a^{\,2})-\tfrac{1}{2}(\vec{\nabla}\varphi_a)^2$$

$$+\bar{\psi}(i\not{\partial}-m)\psi+g\bar{\psi}\vec{\gamma}t^a\psi\cdot\vec{A}_a+\vec{E}_a\cdot\dot{\vec{A}}^a\,, \quad (3.1)$$

where $(\nabla\phi^a)^2$ is given by Eq. (2.15) and the time component of $\bar{\psi}_g t^a\gamma^\mu A_\mu^a\psi$ is contained in $(\vec{\nabla}\phi^a)^2$.

The fermion propagator renormalization consists of two parts: the mass part and the self-energy part. For the former, the pole in the propagator is defined to be at the "physical" mass m_R; that is,

$$S_F^{-1}(p)\big|_{\not p=m_R}=0\,, \quad (3.2)$$

where $S_F(p)$ is the renormalized fermion propagator. However, if confinement occurs, the above procedure is ill defined since the fermion fields in the Lagrangian will not appear in the physical spectrum and the fermion mass parameter will not be a gauge-invariant quantity. Clearly this type of behavior does not happen order by order in per-

turbation theory based on the usual vacuum structure. Furthermore, confinement by a mechanism analogous to that in the Schwinger model[15] implies that mass renormalization is performed by including only the ultraviolet contributions to self-mass corrections and not the infrared components. In Appendix A, these infrared components are related to the longitudinal part of the non-Abelian interaction, as expected in a Schwinger-type mechanism. Below this distinction is ignored since only standard perturbation theory is considered.

The self-energy or wave-function renormalization for the fermion propagator is defined as follows:

$$(d/d\not{p})S_F^{-1}(p)\,|_{p^2-m^2=-\lambda^2}=1\,, \tag{3.3}$$

in which the slightly off-mass-shell point λ^2, $0<\lambda^2 \ll m^2$, and $\lambda\sim\beta m$ ($\beta=v/c$), avoids infrared divergences. The renormalization point for gluon (transverse $\vec{E}^a$ or $\vec{A}^a$ field) and Coulomb propagators is chosen to be at $p^2=-\mu^2$ where $0<\mu^2\ll m^2$ and $\mu\sim\beta m$. Proper vertices are renormalized at the symmetry point (which for the three-point A^a vertex is $p_1^2=p_2^2=p_3^2=-\mu^2$) with the following exception: a Coulomb line (only one if there are several in the vertex) is renormalized at $q=0$. Even though this choice of renormalization point for the Coulomb line is not in the momentum region appropriate to nonrelativistic bound states, which is $q\sim\beta m$, the Ward identities greatly simplify with this choice.

Charge conservation implies a trivial Ward identity for the charge vertex (explicitly the fermion-fermion charge vertex is used, but the argument here is also valid, for example, for the gluon-gluon-charge vertex),

$$Z_1^Q=Z_2\,, \tag{3.4}$$

where Z_1^Q is the renormalization constant of the proper charge vertex and Z_2 is the renormalization constant of the fermion propagator. This Ward identity is true in all gauges but is useful only in the radiation gauge because in it the charge vertex can be related simply to the Coulomb vertex. To find this relation consider the proper vertex

$$\langle 0|\,T^*(\psi(p)\bar{\psi}(p+q)A_a^\mu(q))\,|0\rangle_{1\mathrm{PI}}$$

(1PI = one particle irreducible). For $\mu=1,2,3$ this vertex is the fermion-fermion-gluon vertex and for $\mu=0$ it is the fermion-fermion-Coulomb vertex [with A_a^0 given by Eq. (2.13)]. For the Coulomb vertex 1PI refers to the Coulomb line as given by the perturbation-theory rules in Table I. Furthermore, this Coulomb vertex differs from the charge density vertex,

$$\langle 0|\,T^*(\psi(p)\bar{\psi}(p+q)j_a^0(q))\,|0\rangle_{1\mathrm{PI}}\,,$$

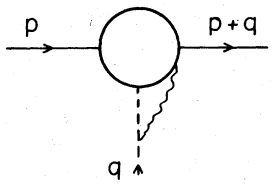

FIG. 1. Difference between Coulomb and charge density vertices, $D(q)$.

by the generalized Coulomb potential $\mathfrak{D}\nabla^2\mathfrak{D}$ [see Eq. (2.15)]. Now define the set of graphs which contribute to the Coulomb vertex but not to the charge vertex as $D(q)$ (where unnecessary indices have been suppressed.). $D(q)$ has the general form given in Fig. 1 which is expressed analytically by

$$\langle 0|\,T^*(\psi(p)\bar{\psi}(p+q)j_a^0(q))\,|0\rangle_{1\mathrm{PI}}+D(q)$$
$$=\langle 0|\,T^*(\psi(p)\bar{\psi}(p+q)A_a^0(q))\,|0\rangle_{1\mathrm{PI}}\,. \tag{3.5}$$

The desired connection between the charge vertex, that is, the charge density vertex at $q=0$, and the Coulomb vertex is established by the following fact:

$$D(0)=0\,. \tag{3.6}$$

The proof of Eq. (3.6) is obtained by showing that $D_i(q)$, defined by $D(q)\equiv q_iD^i(q)$, is finite for $q\neq 0$ and diverges no worse than logarithmically at $q=0$ to any finite order of perturbation theory. When $q\neq 0$, $D_i(q)$ is primitively convergent and therefore no ultraviolet divergences appear as $q\to 0$. However, simple power counting implies a possible linear divergence in the infrared region even when the fermion propagators are slightly off shell ($p^2-m^2=-\lambda^2<0$). Fortunately, a careful study of the numerator structure of the propagators (for example, the transverse projection operators) reduces the actual divergence by one power as $q\to 0$. The details of the proof are given in Appendix A. If Z_1 is defined to be the renormalization constant of the Coulomb vertex, then an immediate consequence of Eqs. (3.4–3.6) is that

$$Z_1=Z_2 \tag{3.7}$$

since renormalization of the Coulomb line is at $q=0$. This Ward identity, also valid in QED, implies that the coupling constant renormalization is given exactly by the Coulomb propagator $[\langle 0|\,T^*(A_a^0A_b^0)\,|0\rangle]$ corrections and therefore the β function, the logarithmic derivative of the coupling constant with respect to the renormalization point, depends only on these Coulomb propagator corrections.

There will also be a Ward identity for the $\vec{A}-\vec{E}$-Coulomb vertex analogous to Eq. (3.7) which implies that the renormalization of this vertex is equal to the $\vec{A}-\vec{E}$ propagator renormalization.

TABLE I. Perturbation theory rules ($P^{\mathrm{Tr}}_{ij}(k)=\delta_{ij}-k_ik_j/\vec{k}^2$).

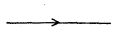	Fermion propagator	$\dfrac{i}{\not{p}-m+i\epsilon}$
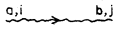	A field propagator	$\dfrac{-iP^{\mathrm{Tr}}_{ij}(k)\delta_{ab}}{k^2+i\epsilon}$
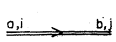	E field propagator	$\dfrac{-i\vec{k}^2P^{\mathrm{Tr}}_{ij}(k)\delta_{ab}}{k^2+i\epsilon}$
	Mixed propagator	$\dfrac{-k^0P^{\mathrm{Tr}}_{ij}(k)\delta_{ab}}{k^2+i\epsilon}$
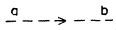	Coulomb force	$\dfrac{-i}{\vec{k}^2}\delta_{ab}$
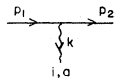	Fermion-A field vertex	$-ig\gamma^i t^a$
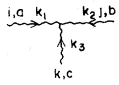	Triple vertex	$-gf^{abc}[\delta^{ij}(k_2-k_1)^k+\delta^{jk}(k_3-k_2)$ $+\delta^{ik}(k_1-k_3)^j]$
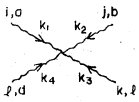	Quartic vertex	$-ig^2[f_{abg}f_{cdg}(\delta^{ik}\delta^{jl}-\delta^{il}\delta^{jk})$ $+f_{acg}f_{bdg}(\delta^{ij}\delta^{kl}-\delta^{il}\delta^{jk})$ $+f_{adg}f_{cbg}(\delta^{ik}\delta^{jl}-\delta^{ij}\delta^{kl})]$
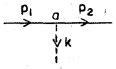	Fermion-Coulomb force	$-ig\gamma^0t^a$
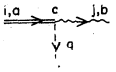	Vector-meson Coulomb force	$igf_{acb}\delta_{ij}$
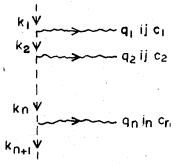	A field emission via Coulomb force	$(-1)(n+1)g^n(f_{ac_1a_1}f_{a_1c_2a_2}\cdots f_{a_{n-1}c_nb})$ $\times(k_2^{i_1}\cdots k_{n+1}^{i_n})\times\begin{cases}1, & n=1\\ \prod_{m=2}^{n}\dfrac{i}{\vec{k}_m^2}, & n>1\end{cases}$

These two Ward identities show that the renormalization of the term $(\nabla\phi^a)^2=j_a^0A_0^a$ in the Lagrangian density is accomplished by coupling-constant renormalization. Finally, there will be the usual Ward identities which insure that the coupling constant is independent of which vertex is used to define its renormalization.

There is another application of Eq. (3.6) which is also related to the charge density. By using a superpotential it is possible to define two charge densities,

$$j_a^0(x)_1=gf_{abc}\vec{E}_b\cdot\vec{A}_c+\psi^\dagger gt^a\psi\,, \tag{3.8a}$$

$$j_a^0(x)_2=gf_{abc}(\vec{E}_b-\vec{\nabla}\varphi_b)\cdot\vec{A}_c+\psi^\dagger gt^a\psi\,, \tag{3.8b}$$

the first defined in terms of the transverse electric field, the second in terms of the full electric field. The difference between these two densities is $\Delta j_a^0(x)$ where

$$\Delta j_a^0(x)=-gf_{abc}\vec{\nabla}\cdot(\varphi^b\vec{A}^c)\,. \tag{3.9}$$

Although $\Delta j_a^0(x)$ is a total divergence, it might contribute to the charge because $\phi^a(x)$ is a nonlocal operator. However, the set of graphs contributing to the Δj_a^0 vertex is the same set which contributes to the Coulomb vertex, the only difference being

the relative weights of individual graphs, as can be seen by comparing the perturbative expansions of Eqs. (2.12) and (2.13). Therefore $D(0)=0$ implies that Δj_a^0 does not contribute to the charge for fermion states with similar arguments applying to other states, and therefore this superpotential does not change the charge operator.

IV. THE FOLDY-WOUTHUYSEN TRANSFORMATION

The Foldy-Wouthuysen procedure consists of a canonical unitary transformation which eliminates the interaction terms between positive- and negative-frequency components of fermion spinors in the Hamiltonian. This reduction is most useful in the nonrelativistic domain; that is, for interactions whose Fourier components are small compared to m, the fermion mass, because in such a case, the positive-frequency parts of the spinors interact negligibly with the negative-frequency parts and an intuitive nonrelativistic picture is valid. For the free Dirac Hamiltonian the Foldy-Wouthuysen transformation can be performed exactly.[4] In the presence of external electromagnetic fields, the Hamiltonian, for a fixed number of fermions, although not transformable exactly, may be put into Foldy-Wouthuysen form to any desired order in a power series in $1/m$ by a sequence of Foldy-Wouthuysen transformations.[5] Here the non-Abelian Hamiltonian is to be transcribed into Foldy-Wouthuysen form in a second-quantized formalism. Therefore pair creation cannot be ignored completely since it contributes in order $1/m^2$. Indeed, because the Foldy-Wouthuysen transformation eliminates pair creation terms in the Hamiltonian, to find all relativistic corrections in order $1/m^2$ it is necessary to calculate the effect of the canonical transformation on the state vectors, but fortunately pair creation terms do not affect the spectrum of states.

A sequence of unitary Foldy-Wouthuysen transformations on the full relativistic Hamiltonian, given in Eq. (2.14b), produces the nonrelativistic Hamiltonian and its first relativistic corrections (with pair creation effects being calculated separately). This procedure is straightforward but tedious and the details are presented in Appendix B. To remove all Dirac operators that connect large and small components of the spinors through order $1/m^2$ requires three canonical transformations. The transformed Hamiltonian H''' may be written as

$$H''' = e^{iS''}e^{iS'}e^{iS}He^{-iS}e^{-iS'}e^{-iS''}$$
$$= mH_{-1}+H_0+(1/m)H_1+(1/m^2)H_2+R\,, \qquad (4.1)$$

where the H_i do not contain any explicit mass dependence, and R, of order $1/m^3$, is unknown except for kinetic energy terms. The Hermitian operators S, S', and S'', generate the Foldy-Wouthuysen transformations to orders 1, $1/m$, and $1/m^2$, respectively, where S and S' are given by (see Appendix A)

$$S=\frac{-i}{2m}\int d^3x\,\psi^\dagger(x)\beta\vec{\alpha}\cdot(-i\vec{\nabla}-gt^a\vec{A}^a)\psi(x), \qquad (4.2a)$$

$$S'=\frac{-1}{4m^2}\int d^3x\,\psi^\dagger(x)\vec{\alpha}gt^a\psi(x)\cdot[\vec{E}^a-\vec{\nabla}A_a^0]\,. \qquad (4.2b)$$

The form of S'' is irrelevant since the Hamiltonian through order $1/m^2$ is independent of it. Below the various terms in the Hamiltonian are listed and described. The fermion mass term is

$$H_{-1}=\int d^3x\,\psi^\dagger(x)\beta\psi(x)\,. \qquad (4.3)$$

The term independent of fermion mass is

$$H_0=\int d^3x\,\tfrac{1}{2}\{[(\vec{E}^a)^2+(\vec{B}^a)^2]+j_a^0A_0^a\}\,. \qquad (4.4)$$

H_0 consists of two terms which, together with the nonrelativistic kinetic energy and H_{-1}, forms the nonrelativistic Hamiltonian. The first of these two terms is the radiation part of the Yang-Mills Hamiltonian and the second is the non-Abelian generalization of the instantaneous Coulomb interaction [j_a^0 and A_a^0 are given in Eqs. (2.9) and (2.13), respectively] identical to Eq. (2.15). Unlike the Abelian theory, this interaction is not a c number. The nonrelativistic kinetic energy is contained in H_1, which is

$$H_1=\int d^3x\,\tfrac{1}{2}(\psi^\dagger\beta D^2\psi+\psi^\dagger\beta\vec{\sigma}gt^a\psi\circ\vec{B}_a)\,, \qquad (4.5)$$

where $D^2\equiv(i\vec{\nabla}+gt_a\vec{A}^a)^2$ and

$$\vec{\sigma}=\begin{pmatrix}\vec{\sigma}_p & 0\\ 0 & \vec{\sigma}_p\end{pmatrix}$$

with $\vec{\sigma}_p$ being the Pauli matrices. H_1 also consists of two parts, the first of which is the canonical nonrelativistic kinetic energy of the fermions in the presence of non-Abelian gauge fields. Therefore the complete nonrelativistic Hamiltonian is

$$H_{\rm NR}=m\int d^3x\,\psi^\dagger\beta\psi+\tfrac{1}{2}\int d^3x\,(\vec{E}_a{}^2+\vec{B}_a{}^2+j_a^0A_0^a)$$
$$+\frac{1}{2m}\int d^3x\,\psi^\dagger\beta D^2\psi\,. \qquad (4.6)$$

The other term in H_1 represents the non-Abelian magnetic dipole interaction. Here the magnetic field includes that produced by the particles themselves, and is not only an external field. H_1 (when iterated) contributes to the fine structure, and in particular it includes the spin-spin and tensor interactions. H_2, the final term calculated, produces the rest of the relativistic fine-structure corrections:

$$H_2 = \tfrac{1}{16}\int d^3x\left[\vec{\mathcal{J}}_+^a\vec{\mathcal{J}}_-^a - \vec{\nabla}\cdot\vec{\mathcal{J}}_+^a\frac{1}{\vec{\nabla}^2}\vec{\nabla}\cdot\vec{\mathcal{J}}_-^a - \int d^3z\,d^3w\,\vec{\nabla}\cdot\vec{\mathcal{J}}_+^a(x)\mathfrak{D}_{ac}(x,z)\vec{\nabla}_z^2\mathfrak{D}_{cb}(z,w)\vec{\nabla}\cdot\vec{\mathcal{J}}_-^b(w)\right]$$
$$+\tfrac{1}{8}\int d^3x\psi^\dagger g t^a\psi\vec{\nabla}^2A_0^a(x)$$
$$+\tfrac{1}{8}\int d^3x\psi^\dagger\left[i\epsilon^{ijk}\sigma^j\left(\frac{2}{i}\partial^k g t^a + \frac{g^2}{2}\{t^a,t^b\}A_b^k\right) + \frac{i}{2}f_{aeb}g^2t^eA_b^i\right]\psi(E_a^i - \partial^iA_a^0)$$
$$+\tfrac{1}{8}\int d^3x\psi^\dagger\left[i\epsilon^{ijk}gt^a\sigma^i\left(\frac{1}{i}\partial^jE_a^k\right)\psi\right], \tag{4.7}$$

where

$$\vec{\mathcal{J}}_\pm^a(x) = \psi^\dagger(x)gt^a\vec{\alpha}\,\frac{1\pm\beta}{2}\psi(x)\,.$$

The first term is a relativistic correction to the fermion interaction due to retardation effects of the non-Abelian vector field in the radiation gauge. This effect is also present classically. The second term, characteristic of the Dirac theory and corresponding in classical electrodynamics to a momentum-dependent interaction of a charged particle with the Coulomb field, is the *Zitterbewegung* and the generalization of the Darwin term. The spin-orbit coupling is included in the third and fourth terms.

In a calculation of matrix elements to order $1/m^2$ appropriate insertions of H_1, H_2, S, and S' must be included. For example, in a given graph these $1/m^2$ corrections might consist of two insertions of H_1 or one insertion of H_2. However, for a calculation of the spectrum of states, insertions of S and S', and therefore fermion pair creation terms, may be ignored since the Foldy-Wouthuysen transformations are unitary. Finally note that in order for this expansion in terms of $1/m$ to be meaningful the parameter m must be the renormalized mass and not the bare mass (see the discussion in Sec. III).

V. VERIFICATION OF THE FOLDY-WOUTHUYSEN TRANSFORMATION

In the preceding section the formal operator expansion of the radiation-gauge Hamiltonian in powers of $1/m$ was presented through order $(1/m)^2$. However, even when all external momentum are restricted to be in the nonrelativistic domain this expansion may fail to give the correct behavior of Green's functions in powers of $1/m$ if loop integrals are dominated by ultraviolet regions of integration. In such a case the large-mass expansion of the Green's function is not directly related to the large-mass operator expansion. The absence of such behavior, which validates the Foldy-Wouthuysen operator expansion in Sec. IV, is guaranteed by the following theorem, an extension of the Appelquist-Carazzone theorem[16]:

For any suitably renormalized Green's function in which all external fermion momenta are in the nonrelativistic domain and in which all external gluon momenta are of the same order of magnitude as the external fermion three momenta, all momentum transfers from fermion lines are effectively the same order of magnitude as the external three momenta, fermion pair creation is negligible, and fermions couple only to Coulomb lines.

To prove this theorem consider an arbitrary graph contributing to any Green's function and isolate the fermion lines which are connected to external fermions. The only contributions in the nonrelativistic limit are those in which the number of external fermions and the number of external antifermions are the same in the initial and final states. In this way, a typical graph may be represented as in Fig. 2. The object B need not be connected and the Green's function may be off the mass shell. By assumption the external fermion momenta p_i are in the region $|\vec{p}_i| \sim \beta m$, $p_i^0 - m \sim \beta^2 m$ ($\beta = v/c \ll 1$) and the external gluon momenta $q_i^\mu \sim \beta m$ To prove the theorem it is sufficient to show that the dominant contribution to any graph comes from the region where all $k_i^\mu \lesssim \beta m$ (all of the k_i are not independent). In Euclidean space an equivalent statement to show is that $(\sum_{i\in S}k_i)^2 \lesssim \beta^2m^2$ for every set S of indices. First assume that this region dominates. Then the Appelquist-Carazzone theorem implies that all loop momenta in B are infrared dominated and that there are no internal fermion loops. Consider any fermion propagator in Fig. 2, which may be written as

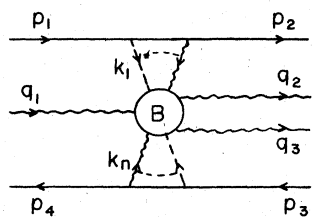

FIG. 2. Isolation of external fermion lines.

$$\frac{\not p - \sum \not k_i + m}{(p^2 - m^2) - 2p \cdot \sum_i k_i + (\sum_i k_i)^2} = \frac{p^0\gamma^0 + O(\beta m)}{-2p^0 \sum_i k_i^0 + O(\beta^2 m^2)} \tag{5.1a}$$

$$\equiv \frac{\gamma^0 \pm 1}{2} \frac{1}{\sum_i k_i^0 + O(\beta^2 m)} \tag{5.1b}$$

where $\pm$ refers to fermions or antifermions. It is clear from Eq. (5.1b) that the only non-negligible fermion couplings (here particle and antiparticle are distinguished) are the fermion-fermion-Coulomb and fermion–antifermion–transverse-gluon ones. The latter interaction produces a transverse gluon propagator with energy of order m by energy-momentum conservation. However, dominant contributions come from the region $\lesssim \beta m$ so that this interaction is negligible, and the only relevant coupling for the fermions is the fermion-fermion-Coulomb vertex which implies that there is no pair creation. Then the Foldy-Wouthuysen transformation gives the correct nonrelativistic Hamiltonian, Eq. (4.6), and it may be used to calculate any nonrelativistic Green's function.

To complete the proof it is necessary to show that the region $k_i \lesssim \beta m$ is the only dominant one in the loop integrations. Consider any region of the k_i in which some subset of all possible invariants is of order m^2 or larger and redefine the loop momenta so that a minimum number of linearly independent integration variables, labeled l_i, are required to be of order m or larger in order that the particular subset of possible invariants is of order m^2 or larger. Let that number be N. The remaining loop momenta, labeled r_j, are small compared to m. Symbolically the integral in this region may be represented as

$$\int_{O(m)}^{\infty} d^4l_1 \cdots d^4l_N \int_0^{O(\beta m)} d^4r_{N+1} \cdots d^4r_n F(r_j, l_i, m) P(l_i, r_j, m)$$

where F is the contribution of the explicit fermion lines and P represents the rest of the graph. Now scale all of the large loop momenta l_i by m; that is, define K_i, $i = 1, \ldots, N$, such that $l_i = K_i m$. The fermion propagators containing only small momenta behave similar to F_S where

$$F_S \sim \tfrac{1}{2}(\gamma^0 \pm 1)\{1/[\textstyle\sum_i r_i^0 + O(\beta^2 m)]\}, \tag{5.2}$$

whereas those containing any large momenta behave similar to $(1/m)F_L$ where

$$(1/m)F_L \sim (1/m)[(\gamma^0 \pm 1) - \textstyle\sum_i K_i]/[2\sum_i K_i^0 + (\sum_i K_i)^2]. \tag{5.3}$$

The term $O(\beta^2 m)$ in the denominator of Eq. (5.2) may be ignored except when it serves as an infrared cutoff for the energy integrations. In such a case the integral's dependence on $\beta^2 m$ will be of the form (excluding logs which are irrelevant for this proof) $(1/\beta^2 m)^k$, $k > 0$. This dependence on $\beta^2 m$ cannot occur for propagators containing large momenta. Furthermore, each large momentum must flow through at least one fermion line and therefore there are a minimum of N fermion propagators of type $(1/m)F_L$. The contribution of this region to the graph can now be written as

$$m^{4N-N} \int_{O(1)}^{\infty} d^4K_1 \cdots d^4K_N (F_L)^N \int_0^{O(\beta m)} d^4r_{N+1} \cdots d^4r_n (F_S)^{n-N} P(mK_i, r_j, m).$$

However, the graphs under consideration are properly renormalized so that all internal integrations are convergent. Therefore the integral of $P(mk_i, l_j, m)$ over $K_1, \ldots, K_N$ must converge in the ultraviolet region and may be written

$$P \sim (1/m^{3N+r})P', \tag{5.4}$$

where r is an integer, even by symmetry, and ≥ 2. Furthermore, by Eq. (5.4) the contribution of this region to the graph is at most

$$\frac{1}{m^2} \int_{O(1)}^{\infty} d^4K_1 \cdots d^4K_N (F_L)^N \times \int_0^{O(\beta m)} d^4r_{N+1} \cdots d^4r_n (F_S)^{N-n} P'$$

In the region in which all $k_i \lesssim \beta m$ each factor of m is accompanied by β or β^2 with $\beta^2 m$ always occurring as a nonpositive power in fermion propagators, as discussed above. The power of these $\beta^2 m$ terms (which do not appear in large-momentum propa-

gators) from the region of integration under consideration is therefore greater than that in the region where all momenta are small. Dimensional arguments now imply that this region is suppressed by at least a factor of β^2, due to the external $1/m^2$ above, with respect to the region in which all $k_i \leq \beta m$ and thus the region $k_i \leq \beta m$ for all loop momenta is the dominant one for any graph.

VI. NONRELATIVISTIC BOUND STATES

In the previous sections a general formalism has been developed for studying any nonrelativistic system of fermions minimally coupled to non-Abelian gauge fields. Now, as a specific example of this formalism, nonrelativistic fermion-anti-fermion bound states will be analyzed in perturbation theory. In particular, threshold bound states will be discussed in detail through two loops and three-fermion bound states will be treated as well. The bound-state spectrum is determined by the nonrelativistic reduction of the Bethe-Salpeter kernel, which will be presented here in order to clarify certain aspects of the perturbation calculations to be done in Sec. VIII. The general formalism is based on that of Schwinger,[17] Bethe,[18] Salpeter,[18,19] and Mandelstam.[20] The fully relativistic inhomogeneous Bethe-Salpeter equation is given by

$$G(x_1,y_2;y_1,x_2)=S_F(x_1,y_2)\otimes S_F(x_2,y_1)$$
$$+\int d^4z_1 d^4z_2 d^4w_1 d^4w_2 [S_F(x_1,z_1)\otimes S_F(z_2,y_2)K(z_1,z_2;w_1,w_2)G(w_1,w_2;y_1,x_2)], \tag{6.1}$$

where

$$S_F(x,y)\equiv\langle 0|T^*(\psi(x)\bar{\psi}(y))|0\rangle$$

is the full fermion propagator,

$$G(x_1,y_2;y_1,x_2)\equiv\langle 0|T^*(\psi(x_1)\psi(x_2)\bar{\psi}(y_1)\bar{\psi}(y_2))|0\rangle$$

is the full four-point fermion-antifermion scattering amplitude and $K(z_1,z_2;w_1,w_2)$ is the Bethe-Salpeter kernel, which is two-particle (fermion-antifermion) irreducible in the s channel. Graphically this equation is given by Fig. 3.

To derive the bound-state equation consider G in the region

$$(x_1^0+y_2^0)\gg(y_1^0+x_2^0), \tag{6.2a}$$

$$|x_1^0-y_2^0|\ll|x_1^0+y_2^0-x_2^0-y_1^0|, \tag{6.2b}$$

$$|x_2^0-y_1^0|\ll|x_1^0+y_2^0-x_2^0-y_1^0|, \tag{6.2c}$$

in which $G(x_1,y_2;y_1,x_2)$ is denoted G_+. For G_+ the time scale between initial and final states is much larger than the time scales of either state. Insertion of a complete set of states between the initial and final fermion-antifermion fields in G_+ allows the isolation of the contribution of bound states. In particular, consider a bound state of mass M_B, momentum $\vec{P}$, and energy $E_B=(M_B{}^2+\vec{P}^2)^{1/2}$ which is described by a bound-state wave function $\chi^B(x,\vec{P})$ as follows:

$$\chi^B(x,\vec{P})=\langle 0|T^*(\psi(x/2)\bar{\psi}(-x/2))|B,\vec{P},M_B\rangle. \tag{6.3}$$

Then, translational invariance and the fact that the bound state contributes only when $(x_1^0+y_2^0)>(y_1^0+x_2^0)$ gives for G_+ the form below after transforming the center-of-mass coordinate,

$$G_+(x,y,\vec{P},P^0)=\frac{-i}{P^0-E_B+i\epsilon}\frac{\chi^B(x,\vec{P})\bar{\chi}^B(y,\vec{P})}{2E_B}$$
$$+\text{terms regular as } P^0\to E_B, \tag{6.4}$$

where $x=(x_1-y_2)$ and $y=(y_1-x_2)$. It has been assumed here that the bound state is nondegenerate. To proceed from the inhomogeneous equation for G to the homogeneous bound-state equation for χ^B, note that Eq. (6.4) implies that

$$i\int d^4y\, 2E_B \lim_{P_0\to E_B}(P^0-E_B)G(x,y,\vec{P},P^0)\chi^B(y,\vec{P})$$
$$=\chi^B(x,\vec{P}) \tag{6.5}$$

The orthonormality of χ^B and $\bar{\chi}^B$ has been used here. Similarly, projecting onto the bound state $\chi^B(x,\vec{P})$ in Eq. (6.1) and expressing the result in momentum space gives

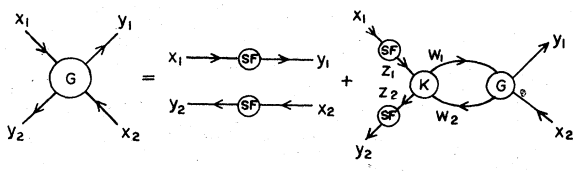

FIG. 3. Inhomogeneous Bethe-Salpeter equation.

$$\chi^B(k,P)=\int\frac{d^4k_2}{(2\pi)^4}S_F\left(k_1+\frac{P}{2}\right)\otimes S_F\left(k_1-\frac{P}{2}\right)K(k_1,k_2;P)\chi^B(k_2,P). \tag{6.6}$$

Equation (6.6) is the fully relativistic bound-state wave equation with irreducible kernel K.

To obtain the nonrelativistic limit, it is convenient to work in the center-of-momentum frame $\vec{\mathbf{P}}=0$ so that $P^\mu=(\vec{0},M)$. In this frame the operator

$$\gamma^0 S_F^{0-1}(k_1+p/2)\otimes S_F^{0-1}(k_1-p/2)\gamma^0$$

is applied to both sides of Eq. (6.6) (S_F^0 is the free fermion propagator):

$$\left[\left(\frac{M}{2}+k_1^0\right)-(\vec{\alpha}\cdot\vec{k}_1+\beta m)\right]\otimes\left[\left(-\frac{M}{2}+k_1^0\right)-(\beta m-\vec{\alpha}\cdot\vec{k}_1)\right]\chi^B(k_1,M)=\int\frac{d^4k_2}{(2\pi)^4}T(\vec{k}_1,\vec{k}_2;k_1^0,k_2^0,M)\chi^B(k_2,M), \tag{6.7a}$$

where (with explicit indices)

$$T^{ln}_{ij}(\vec{k}_1,\vec{k}_2;k_1^0,k_2^0,M)=\left\{\delta_i^{i'}\delta_j^{j'}+\left[\Sigma\left(k_1+\frac{P}{2}\right)S_F\left(k_1+\frac{P}{2}\right)\right]^{i'}_{i}\left[\Sigma\left(k_1-\frac{P}{2}\right)S_F\left(k_1-\frac{P}{2}\right)\right]^{j'}_{j}\right\}K^{ln}_{i'j'}(k_1,k_2;M). \tag{6.7b}$$

This equation may be represented as

$$\chi_B(k,M)=S_F^0(k_1+\tfrac{1}{2}P)\gamma^0\otimes\gamma^0 S_F^0(k_1-\tfrac{1}{2}P)\times\int\frac{d^4k_2}{(2\pi)^4}T(\vec{k}_1,\vec{k}_2;k_1^0,k_2^0,M)\chi^B(k_2,M). \tag{6.8}$$

To obtain a nonrelativistic equation from Eq. (6.8) it is necessary to make the following fundamental assumption: the basic interactions occur over a time scale small compared to the inverse of the energy spread of the wave function. Explicitly, this assumption is that over the range of k_1^0 and k_2^0 for which $\chi^B(\vec{k}_1,k_1^0,M)$ and $\chi^B(\vec{k}_2,k_2^0,M)$ are significantly different from zero, $T(\vec{k}_1,\vec{k}_2;k_1^0,k_2^0,M)$ is approximately constant in the variables k_1^0 and k_2^0. Therefore T may be decomposed into two parts,

$$T=T^0+T', \tag{6.9}$$

where T^0 is instantaneous and T', which contains all the k_1^0 and k_2^0 dependence of T, is small in the sense that it is possible to make a perturbative expansion of Eq. (6.8) in powers of T'. Substituting Eq. (6.9) into Eq. (6.8) and iterating with respect to T' gives

$$\chi^B(k_1,M)=S_F^0(k_1+\tfrac{1}{2}P)\gamma^0\otimes\gamma^0 S_F(k_1-\tfrac{1}{2}P)\times\frac{1}{1-T'S_F^0\gamma^0\otimes\gamma^0S_F^0}\,T^0\chi^B, \tag{6.10}$$

in which the appropriate four-dimensional integrals are to be performed when the denominator is expanded in a power series in T'. In terms of the nonrelativistic wave function $\phi(\vec{k})$, given by

$$\phi(\vec{k})=\int\frac{dk^0}{2\pi}\chi^B(\vec{k},k^0,M), \tag{6.11}$$

Eq. (6.10) becomes

$$\phi(\vec{k}_1)=\int\frac{dk_1^0}{2\pi}S_F^0(k_1+\tfrac{1}{2}P)\gamma^0\otimes\gamma^0S_F^0(k_1+\tfrac{1}{2}P)\times\frac{1}{1-T'S_F^0\gamma^0\otimes\gamma^0S_F^0}\,T^0\phi \tag{6.12}$$

where the last integration is only over the spatial components of the momentum. This exact equation provides a convenient representation of the kernel for quasistatic systems. To extract the large components of the wave function $\phi(\vec{k})$ it is useful to use the following projection operators:

$$P_\pm^0(k_1)\equiv[E_a(k_1)\pm H_a(k_1)]\frac{1}{2E_a(k_1)},$$
$$H_a=\vec{\alpha}\cdot\vec{k}_a+\beta M, \tag{6.13}$$

in terms of which the bound-state wave function may be decomposed as follows (a = fermion index, b = antifermion index):

$$\chi^B(\vec{k}_1,k_1^0,M)=P_+^aP_-^b\chi_{+-}+P_+^aP_+^b\chi_{++}+P_-^aP_-^b\chi_{--}+P_-^aP_+^b\chi_{-+}. \tag{6.14}$$

However, in the nonrelativistic limit $H_a(k_1)\approx E_a(k_1)$ for fermions and $H_b(k_1)\approx -E_b(k_1)$ for antifermions. Therefore only χ_{+-} is large in this limit and the nonrelativistic wave function $\psi(\vec{k})$ is defined by

$$\psi(\vec{k}_1)=\int\frac{dk_1^0}{2\pi}P_+^aP_-^b\chi_{+-}, \tag{6.15}$$

so that for the large nonrelativistic components Eq. (6.12) now becomes approximately

$$\psi(\vec{k}_1)=\int \frac{dk_1^0}{2\pi}\,\frac{1}{M/2-E_a+k_1^0+i\epsilon}\,\frac{1}{M/2-E_b+k_1^0-i\epsilon}\,\frac{1}{1-T'(M/2-E_a+k^0+i\epsilon)^{-1}(M/2-E_b+k^0-i\epsilon)^{-1}}\,T^0\psi\,. \quad (6.16)$$

Now consider Eq. (6.16) when T' is zero, as in nonrelativistic QED. Then

$$(M-E_a-E_b)\psi(\vec{k}_1)=\int \frac{d^3k_2}{(2\pi)^3}\,T^0(\vec{k}_1,\vec{k}_2)\psi(\vec{k}_2). \quad (6.17)$$

In the nonrelativistic limit for the left-hand side of Eq. (6.17),

$$M-E_a-E_b=-E_B-k^2/2\mu \quad (6.18)$$

with E_B = binding energy and $\mu=m_am_b/(m_a+m_b)$. Therefore Eq. (6.17) is the nonrelativistic Schrödinger equation with a possibly nonlocal potential given by $T^0(\vec{k}_1,\vec{k}_2)$.

The most important application of Eq. (6.16) is when $T'\neq 0$ but the lowest-order perturbative expression for T is instantaneous as is the case in QCD. Then to any order of perturbation theory only a finite number of iterations of T' contributes, and the nonrelativistic kernel $K(\vec{k}_1,\vec{k}_2)$ is given by

$$K(\vec{k}_1,\vec{k}_2)=\left[(M-E_a-E_b)\int \frac{dk_1^0}{2\pi}\,\frac{1}{M/2-E_a+k_1^0+i\epsilon}\,\frac{1}{M/2-E_b+k_1^0-i\epsilon}\right.$$

$$\left.\times\frac{1}{1-T'(M/2-E_a+k^0+i\epsilon)^{-1}(M/2-E_b+k^0-i\epsilon)^{-1}}\,T^0\psi\right]_{M-E_a-E_b=0}. \quad (6.19)$$

If the limit $M-E_a-E_b\to 0$ does not exist in the above above expression there is no self-consistent static potential. The terms in this equation involving iterations of T' are not iterations of the nonrelativistic kernel but contribute an amount of the same order and form as T^0 alone. Such terms exist when the nonrelativistic (or static) limit of iterations of the relativistic kernel is not equal to iterations of the nonrelativistic kernel itself. Thus the nonrelativistic kernel is not given by T^0 but by Eq. (6.19) which equals T^0 only when $T'=0$. Use of this kernel produces the correct nonrelativistic bound-state spectrum and all contributions to the nonrelativistic kernel may now be classified as

(a) two-fermion irreducible graphs,

(b) initial state self-energy corrections [see Eq. (6.7b)],

(c) nonrelativistic limit of kernel iterations not iterations of the nonrelativistic kernel [see Eq. (6.19)].

In QCD nonrelativistic bound states are described by the Foldy-Wouthuysen transformed Hamiltonian, Eq. (4.6). In particular only threshold bound states are being considered here and for such states the binding energy $\epsilon\sim\beta^2m$, the same order of magnitude as the kinetic energy. In QED the nonrelativistic kernel is simply the single Coulomb exchange so that a bound state is built solely from the momentum dependence of iterations of the kernel with $\alpha/\beta\sim 1$. If α is small, as in QED, all bound states are threshold, but for large α, β need not be small and the bound states need not be threshold. Since here the nonrelativistic kernel is not a single Coulomb exchange, the requirements on the coupling constant for threshold bound states are more complicated than in QED.

Furthermore, in order to produce nonrelativistic bound states, the Bethe-Salpeter kernel must become effectively instantaneous but the limitation of loop momenta shown in Sec. V does not guarantee an instantaneous kernel. More specifically, if ΔT is the time scale over which the interactions in the kernel occur, then an instantaneous potential is found when $\Delta T\ll 1/\epsilon\sim 1/\beta^2m$ ($1/\epsilon$ is the time scale of motion inside the bound state; i.e., the scale over which the fermions appear free). The kernel must "see" the quarks as free and essentially at rest. This requirement is expressed by $\epsilon(\sim\beta^2m)\ll$ effective loop energy ($\lesssim\beta m$ as shown in Sec. V). Another way of understanding the criterion is as the requirement that most

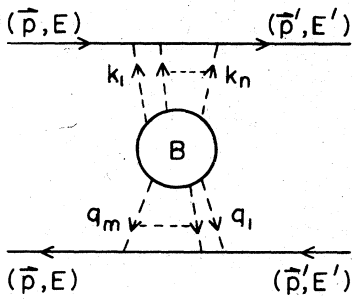

FIG. 4. Nonrelativistic Bethe-Salpeter kernel.

of the time the bound state is simply $q\bar{q}$ (q a quark). In old fashioned perturbation theory, $q\bar{q}$ intermediate states must have energy denominators much smaller than those for $q\bar{q}$+ gluons, or more precisely,

$$\frac{\text{denominator for } q\bar{q}}{\text{denominator for } (q\bar{q}+\text{ gluons})} \xrightarrow[\beta\to 0]{} 0 .$$

As verified in Sec. VII, this requirement is satisfied explicitly for the sum of graphs through two loops in singlet states only, although not true graph by graph. Problems occurring in higher loops are mentioned in Sec. VIII.

The general expression for K in Eq. (6.19) in the non-Abelian theory may be cast into a simple form. Since only Coulomb lines interact with the fermions the nonrelativistic kernel is given by (see Fig. 4)

$$K=\int \frac{d^4k_1}{(2\pi)^4}\cdots\frac{d^4k_{n-1}}{(2\pi)^4}\,\frac{d^4q_1}{(2\pi)^4}\cdots\frac{d^4q_{m-1}}{(2\pi)^4}V_+^{q_1\cdots a_n}(k_1^0,\ldots,k_n^0)B_{b_1^1\cdots b_m^{a_n}}V_-^{b_1\cdots b_m}(q_1^0,\ldots,q_m^0), \tag{6.20a}$$

with

$$V_\pm^{a_1\cdots a_n}(k_1^0,\ldots,k_n^0) = \frac{\gamma^0\pm 1}{2}g^n\frac{t^{a_1}\cdots t^{a_n}}{k_1^0(k_1^0+k_2^0)\cdots(k_1^0+\cdots+k_n^0)}. \tag{6.20b}$$

the form of $V_\pm^{a_1\cdots a_n}$ is an immediate consequence of Eq. (5.16) and

$$B_{b_1^1\cdots b_m^{a_n}}(k_1,\ldots,k_n;q_1,\ldots,q_m)$$

is the appropriate $(n+m)$-point Coulomb function with only Yang-Mills interactions internally ($\sum_1^n k_i=\sum_1^m q_i=p'-p$). This form is reminiscent of the eikonal approximation in that the incoming fermion and antifermion "scatter" several times, each scattering process involving the exchange of only a small fraction of the total energy. Also, in the nonrelativistic limit all of the fermion scattering processes occur at the same point in space (the fermions are at rest) so that the fermion has become an effective external source of soft Coulomb lines with vertices given by Eq. (6.20a).

VII. PERTURBATION THEORY

The spectrum of nonrelativistic fermion antifermion bound states in a non-Abelian gauge theory is determined by the kernel given by Eq. (6.20) (shown in Fig. 5) in which the appropriate kinematic region is $p_i^2-m^2$, t, and $s-4m^2$ all of order $\beta^2m^2\ll m^2$ (s,t are the Mandelstam variables). In this Section a thorough perturbative analysis of the kernel is made through two loops, and in addition three-fermion bound states are discussed. Moreover, since nonrelativistic calculations are easily performed in old-fashioned perturbation theory, the analysis here will be performed in this formalism and the graphs in this section are therefore not covariant but represent a particular time ordering with time increasing from left to right. The initial fermion-antifermion state may be either in the singlet or in the adjoint representation of the gauge group SU(N), the fermions being in the fundamental representation. To lowest order only the single Coulomb exchange, shown in Fig. 5, contributes to the kernel which is

$$k_0=\begin{cases} ig^2T_2\delta_{\lambda_1\lambda_1'}\delta_{\lambda_2\lambda_2'}\left(\dfrac{1}{-t}\right), & \text{singlet} \\ ig^2(T_2-\frac{1}{2}C_2)\delta_{\lambda_1\lambda_1'}\delta_{\lambda_2\lambda_2'}\left(\dfrac{1}{-t}\right), & \text{adjoint.}\end{cases} \tag{7.1}$$

λ and λ' are the diagonal spin indices which will be suppressed below, and $-t=(\vec{p}-\vec{p}')^2$ in the center-of-mass frame. The constants T_2 and C_2 associated with the gauge group are defined by $\sum_a t^a t_a\equiv T_2 1$ where t^a are the fermion representation matrices and $\sum_a T^a T_a\equiv C_2 1$ where T^a are the adjoint representation matrices given by $(T_a)_{bc}\equiv if_{abc}$, f_{abc} being the structure constants of the group. Here, $T_2=(N^2-1)/2N$ and $(T_2-\frac{1}{2}C_2)=-1/2N$ so that, as is well known, the adjoint representation is repulsive with respect to the singlet. For large N the singlet-state group factor $T_2\approx N/2$, N^2 larger than the adjoint-state factor.

In one loop the only contributions to the kernel are the two graphs shown in Fig. 6. Here $q=p-p'$ and k is the loop momentum. The first graph, Fig. 6(a), is exactly instantaneous whereas the transverse gluon loop contribution contains a noninstantaneous part negligible in the one-loop kernel. This transverse gluon loop, as shown in Fig. 6(b) represents the sum of two graphs in the first-

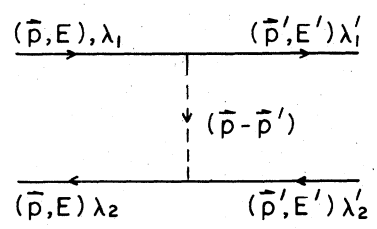

FIG. 5. Single Coulomb exchange.

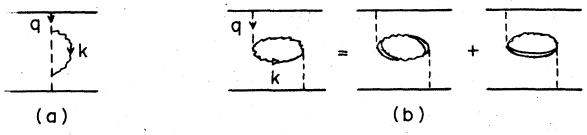

FIG. 6. One-loop graphs contributing to nonrelativistic kernel.

order formalism: the first being two mixed $\vec{A}-\vec{E}$ propagators and the second an $\vec{A}$ and an $\vec{E}$ propagator. Also, another time ordering in which the antifermion emits the Coulomb line before the fermion absorbs it must be included in the kernel. Below it is assumed that all appropriate time orderings have been added to the graphs shown to produce the kernel. It is also clear that to this order the only corrections to the kernel are Coulomb line corrections. These graphs are calculated explicitly in Appendix C by dimensional regularization methods which are useful in two loops. The calculations have been performed previously by different methods.[21] The result for the kernel through one loop is

$$K_1=\frac{ig^2(\mu)}{-t}\left(1-\frac{11}{3}\frac{g^2(\mu)}{16\pi^2}C_2\ln\frac{-t}{\mu^2}\right)\times\begin{cases}T_2, & \text{singlet}\\ T_2-\frac{1}{2}C_2, & \text{adjoint}\end{cases}\tag{7.2}$$

μ is the renormalization point (see Sec. III). The second term in Eq. (7.2), the one-loop contribution, increases the strength of the interaction at large distances as expected in an asymptotically free theory. However, the noninstantaneous graph in Fig. 6(b) must decrease the interaction since it produces QED-type vacuum polarization.[7,14] The instantaneous graph is responsible for the asymptotic freedom effects and dominates the other graph. Also, to order g^4 the renormalization group equation for the coupling constant gives the following result based on the well-known value of the β function in one loop (which is gauge independent):

TABLE II. Two-loop graphs relevant for the Bethe-Salpeter kernel.

	Graph	Renormalized amplitude	Group structure constants (S = singlet, A = adjoint)
(a)	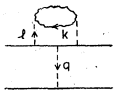	$\frac{ig^2}{-t}G_{S,A}\frac{g^4}{8(2\pi)^4}(2\pi^2-\frac{56}{3})\left(\frac{\epsilon_1\ln(\epsilon_1^2/\lambda^2)-\epsilon_2\ln(\epsilon_2^2/\lambda^2)}{2(\epsilon_2-\epsilon_1)}+1\right)$	$G_S=T_2C_2(T_2-\frac{1}{2}C_2)$ $G_A=C_2(T_2-\frac{1}{2}C_2)^2$
(b)	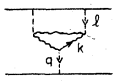	$\frac{ig^2}{-t}(2G_{S,A})\frac{g^4}{8(2\pi)^4}\left[(2\pi^2-\frac{56}{3})\frac{1}{2}\ln\frac{q^2}{\lambda^2}+B\right]$	$2G_S=-\frac{1}{2}T_2C_2^2$ $2G_A=-\frac{1}{2}C_2^2(T_2-\frac{1}{2}C_2)$
(c)	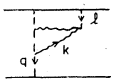	$\frac{ig^2}{-t}(2G_{S,A})\frac{g^4}{8(2\pi)^4}C$	$2G_S=-\frac{1}{2}T_2C_2^2$ $2G_A=-\frac{1}{2}C_2^2(T_2-\frac{1}{2}C_2)$
(d)	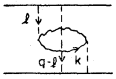	$\frac{ig^2}{-t}G_{S,A}\frac{g^4}{8(2\pi)^4}\left[(2\pi^2-\frac{56}{3})\left(\frac{\epsilon_1\ln(\epsilon_1^2/q^2)-\epsilon_2\ln(\epsilon_2^2/q^2)}{2(\epsilon_1-\epsilon_2)}-1\right)+D\right]$	$G_S=T_2C_2(T_2-\frac{1}{2}C_2)$ $G_A=C_2(T_2-\frac{1}{2}C_2)(T_2-C_2)$
(e)	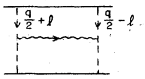	$\frac{ig^2}{-t}G_{S,A}\frac{g^4}{8(2\pi)^4}E$	$G_S=\frac{1}{4}T_2C_2^2$ $G_A=-\frac{1}{4}C_2^2(T_2-\frac{1}{2}C_2)$
(f)	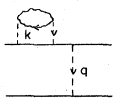	$\frac{ig^2}{-t}G_{S,A}\frac{g^4}{8(2\pi)^4}\left((2\pi^2-\frac{56}{3})\frac{1}{2}\ln\frac{\epsilon_1^2}{\lambda^2}\right)$	$G_S=T_2^2C_2$ $G_A=C_2T_2(T_2-\frac{1}{2}C_2)$
(g)	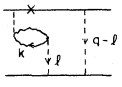	$\frac{ig^2}{-t}G_{S,A}\frac{g^4}{8(2\pi)^4}\left((2\pi^2-\frac{56}{3})\frac{1}{2}\ln\frac{q^2}{\epsilon_1^2}-D\right)$	$G_S=T_2^2C_2$ $G_A=C_2(T_2-\frac{1}{2}C_2)^2$

$$g^2(\mu)-\frac{11}{3}\frac{g^4(\mu)}{16\pi^2}C_2\ln\frac{-t}{\mu^2}=g^2(-t). \tag{7.3}$$

The value of the β function in Eq. (7.3) is that for a pure Yang-Mills theory since fermions are negligible nonrelativistically. Furthermore, Eqs. (7.2) and (7.3) show that the coupling constant renormalization is given exactly by the Coulomb propagator renormalization, as required by the Ward identity $Z_1=Z_2$ proven in Sec. III and Appendix A. The kernel through one loop may now be written as

$$K_1=\frac{ig^2(-t)}{-t}\times\begin{cases}T_2, & \text{singlet}\\ T_2-\frac{1}{2}C_2, & \text{adjoint}.\end{cases} \tag{7.4}$$

Next, for the two-loop kernel, there are several important contributions. Consider first Coulomb propagator corrections. These terms effect the change of the coupling constant from $g^2(-\mu)$ to $g^2(-t)$ as a consequence of the Ward identity proved in Sec. III, that $Z_1=Z_2$. Therefore, these graphs may be used to calculate the β function to two loops in the Coulomb gauge. The value of the leading log contributions to the β function in each order are just iterations of the value of the one-loop kernel since the β function itself is expressible as a power series in $g^2(-t)$ alone. In fact, the Ward identities clarify cancellations of some leading log contributions. Consider for example the two-loop irreducible corrections to Fig. 6(b) consisting of graphs which are either gluon-gluon-Coulomb vertex corrections or gluon propagator corrections. The Ward identity $Z_1=Z_2$ applies to the gluon propagator as well as to the fermion propagator, so that the leading divergences of these graphs must cancel by themselves.

All contributions to the two-loop kernel except the Coulomb line corrections, discussed above, are shown in Table II. The details of the calculation of graph (a) are presented in Appendix C, the calculation of the other graphs being similar. λ is the fermion renormalization point (see Sec. III) and $t=-q^2$. At the two-loop level it is necessary to specify the initial and final states more carefully than previously by distinguishing between ϵ_1 and ϵ_2, the amounts by which these two states are off shell, respectively, with $\epsilon_1\neq\epsilon_2$ and $\epsilon_1,\epsilon_2\sim\beta^2 m$. The kernel must be effectively independent of both these parameters. B, C, D, and E are numerical constants. In addition there are, of course, similar graphs with fermion and antifermion lines interchanged. Graph (f) is an external fermion self-energy correction which is included in the kernel for the initial state only and graph (g) is a two-fermion reducible contribution due to the energy dependence of the kernel as discussed in the preceding section. For the fully relativistic kernel this graph would be an iteration of the one-loop kernel with the zero-loop kernel, but it is not an iteration nonrelativistically. To see explicitly how this contribution arises consider the energy denominator of the intermediate state with two gluons:

$$(|\vec{k}|+|\vec{l}-\vec{k}|+\epsilon_1)^{-1}=(|\vec{k}|+|\vec{l}-\vec{k}|)^{-1}-(|\vec{k}|+|\vec{l}-\vec{k}|)^{-1}\epsilon_1(|\vec{k}|+|\vec{l}-\vec{k}|+\epsilon_1)^{-1}. \tag{7.5}$$

The second term, a relativistic correction for the one-loop kernel, combines with the energy denominator of the two-fermion intermediate state, ϵ_1^{-1}, to produce a contribution to the two-loop kernel of the same order of magnitude as the other graphs in Table II. The X on the fermion line indicates that the second term in Eq. (7.5) is to be used for the energy denominator in the appropriate intermediate state.

The logarithmic dependence on the fermion renormalization point λ in graph (f) cancels with the λ dependence in the vertex correction graphs (a) and (b) for both singlet and adjoint states. This result is a verification in two loops of the Ward identity $Z_1=Z_2$. Graph (c) is a finite graph unrenormalized since it is a graph in the fermion-Coulomb vertex not part of the fermion charge vertex, as explained in Sec. III. Also the dependence on the off shellness, ϵ_1 and ϵ_2, which is similar to an infrared or large time cutoff, cancels pairwise between graphs (a) and (d), and between graphs (f) and (g), but only for the singlet state. The two graphs in each pair are distinguished by a Coulomb line being absorbed on a fermion or antifermion line. Since the bare instantaneous Coulomb line at zero momentum couples only to the charge operator, the sum of the graphs in each pair is the total charge in the state, zero only for the singlet. This observation is also the basis of the Ward identity $Z_1=Z_2$ so that cancellation of infrared and ultraviolet divergences both are due to the same effect. Adding all of the contributions indicated in Table II gives for the kernel through two loops

$$K_2=\begin{cases}\dfrac{ig^2(-t)}{-t}T_2\left[1+bC_2\dfrac{g^4(-t)}{8(2\pi)^4}\right], & \text{singlet}\\[2ex] \dfrac{ig^2(-t)}{-t}(T_2-\frac{1}{2}C_2)\left[1+bC_2\dfrac{g^4(-t)}{8(2\pi)^4}-\frac{1}{2}C_2\dfrac{g^4(-t)}{8(2\pi)^4}\left(2\pi^2-\dfrac{56}{3}\right)\left(1-\dfrac{\epsilon_2}{\epsilon_2-\epsilon_1}\ln\dfrac{\epsilon_2}{\epsilon_1}\right)\right], & \text{adjoint},\end{cases} \tag{7.6}$$

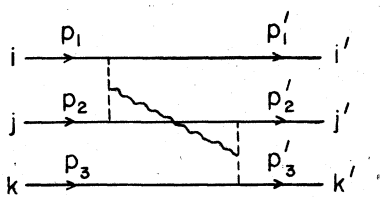

FIG. 7. Nonzero contribution to three-body kernel in two loops.

where[22] $b \sim 20$. For the singlet state only, the kernel in Eq. (7.6) gives a static nonrelativistic potential valid in the infinite-mass limit. The energy dependence of the kernel for the adjoint representation does not permit a self-consistent nonrelativistic limit to be obtained. Note that this distinction between the singlet and nonsinglet only applies to the kernel where $\epsilon_1 \neq \epsilon_2$. For on- or off-shell matrix elements $\epsilon_1 = \epsilon_2$ so that the third term of the kernel for the nonsinglet state vanishes and the remaining terms are the same as the singlet with the change, as is valid in lower orders, $T_2 \to T_2 - \frac{1}{2}C_2$.

For three-fermion bound states, qualitatively the same structure will emerge as in the fermion-antifermion case since the form of the kernel is determined by the Ward identities and the identification of the charge operator. However, the kinematics is more complicated and a simple form as in Eq. (7.6) has not been obtained so that only some general features are described here. The projection operator onto the singlet sector is $\frac{1}{6}\epsilon_{ijk}$ (i,j,k are group indices). Also, there are three possible momentum transfers $\vec{q}_{ij}^{\,2} = (\vec{p}_i - \vec{p}_j)^2$ where $i,j = 1,2,3$, and the energy denominator for the three-fermion state is $(M - E_1 - E_2 - E_3)$ for either the two-body or three-body kernel. Below sixth order the kernel is the sum of the three two-body kernels, each of which is similar to the fermion-antifermion kernels. However, in sixth order there are contributions to the three-body kernel, such as the graph shown in Fig. 7, which contributes a finite amount to the kernel. Furthermore cancellation of the infrared divergences requires terms from both the two-body and three-body kernels, as can be seen from the graphs shown in Fig. 8. The first two graphs, 8(a) and 8(b) are two-body contributions but this sum still depends on the binding energy. Only when graph 8(c), a three-body contribution, is added does the cancellation occur since the final Coulomb line, which gives a measure of the charge in the infrared limit, must be attached to each fermion line in order to give cancellation in the singlet states. However, in order to obtain this cancellation the bound-state wave function must be attached to the final state and the resulting integrations performed explicitly. Therefore the three-body kernel not only cannot be neglected, but also is necessary in order to obtain a static potential.

VIII. DISCUSSION AND CONCLUSIONS

In this paper a consistent general formalism has been developed for describing nonrelativistic systems of fermions minimally coupled to Yang-Mills fields. The application of this nonrelativistic formalism to bound states produced a kernel which has several interesting characteristics. First, the nonrelativistic potential is not simply the instantaneous part of the relativistic kernel, as it is in QED, but has a more intricate structure involving terms which relativistically are iterations of the kernel. A perturbative analysis through two loops in the radiation gauge distinguished group singlet states by the fact that only for these states does a nonrelativistic potential exist. Also the effective strength of the coupling constant is determined by the pure Yang-Mills theory at a momentum value typical of the momentum transfers in the bound state. Finally, the nonrelativistic potential is completely spin independent even though its Lorentz structure is complicated.

Three-loop contributions to the kernel apparently produce $\log \epsilon$ terms even in the singlet channel, as, for example, in the graph shown in Fig. 9. Whether this energy dependence cancels with other three-loop graphs is not known at present. If one sums the contributions of all possible numbers of Coulomb lines at intermediate times in the graph, then the energy dependence becomes negligible.[7]

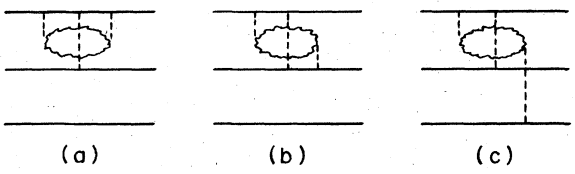

FIG. 8. Cancellations of divergences in the three-fermion kernel.

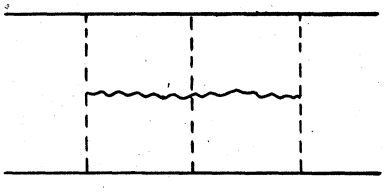

FIG. 9. Three-loop contribution to the kernel with $\log\epsilon$ dependence.

A similar process occurs in Lamb-shift calculations but the Lamb shift is a relativistic correction whereas Fig. 9 is a nonrelativistic contribution. Although this resummation of the perturbation expansion removes this energy dependence in three loops, a consistent scheme to eliminate such energy dependences valid in higher orders of perturbation theory has not been found.

The Foldy-Wouthuysen transformations which produced the nonrelativistic Hamiltonian, Eq. (4.6), also give the structure of the first relativistic corrections. These terms lead to effective interactions for energy shifts and splittings in two-fermion bound states analogous to the Breit-Fermi interactions in QED. Presently the possible phenomenological implications of these terms in J/ψ and Υ systems are under investigations.[23]

The perturbative analysis of Sec. VII is valid for weak fields with the naive vacuum structure although nonperturbative effects may make major modifications in the bound-state spectra. However, the radiation gauge Hamiltonian formalism developed in this paper can serve as a convenient starting point for a nonperturbative analysis in the nonrelativistic limit of gauge ambiguities[14,24] or of multiple-vacua phenomena.

ACKNOWLEDGMENTS

The author would like to thank the physics department at Yale University, where part of this manuscript was written, for its hospitality. He would in particular like to thank T. Appelquist, A. Chodos, M. Dine, and C. Sommerfield for numerous informative conversations. Finally he would like to thank the Laboratory for Nuclear Science and the Center for Theoretical Physics at the Massachusetts Institute of Technology for their aid and assistance in this research. This work was supported in part by the Department of Energy under Contract No. EY-76-C-02-3069-*000.

APPENDIX A: PROOF OF THE WARD IDENTITY

In this appendix a proof is given of Eq. (3.5), $D(0)=0$, and in fact it is shown that $D(q)\xrightarrow[q\to 0]{} q\ln^n q$. The external fermions are assumed to be off mass shell by an amount $p^2-m^2=-\lambda^2\sim 2m\epsilon$ where here, unlike in Sec. VII, $\epsilon \gg q$. Furthermore, old-fashioned (time-ordered) perturbation theory is used throughout. As $q\to 0$, the only possible divergences that arise are infrared divergences since clearly this limit cannot introduce ultraviolet divergences. Any possible divergence at a finite value of the loop momenta can be shifted to zero by a suitable redefinition of the appropriate loop momenta.

The method of the proof is as follows: All possible sets of subintegrations for each graph in $D(q)$ are classified and examined to show for each one $D(q)$ is finite as $q\to 0$. In particular, it is shown that $D_i(q)$ $[D(q)\equiv q^i D_i(q)]$ is finite as $q\to 0$ except for possible log divergences. Note that for examination of each particular set of subintegrations, all other loop momenta can be considered finite and fixed. Then each graph in $D_i(q)$ will diverge no worse than logarithmically if no set of subintegrations diverges worse than logarithmically. In the proof below dimensions will always refer to $D_i(q)$. Each set of subintegrations forms a subgraph with fixed finite external momenta (except possibly q). These subgraphs are divided into three classes as follows:

(1) No linear combination of external momenta equals q; i.e., no linear combination goes to zero as $q\to 0$ except clearly the sum of all the momenta which is identically zero.

(2) There is a linear combination of the external momenta which equals q. However, the first interaction vertex of the external Coulomb line, the Coulomb-Coulomb-gluon vertex explicitly shown in Fig. 2, does not appear. This vertex will be called the distinguished vertex below.

(3) The distinguished vertex does appear in the subgraph.

The proof of case (1) shows that there are no infrared divergences for any graph at nonexceptional momenta, a fact which is known, but the proof here is constructed so as to facilitate the proof in cases (2) and (3).

The basis of the proof is an infrared power counting argument. Consider the region of loop momenta in a subgraph which is much smaller than any of the external momenta (except $q\to 0$). In this region scale all loop momenta by λ, which scales the subgraph by λ^d where d is the infrared dimension of the graph and if $d\geq 0$, the subintegral diverges at most logarithmically in the infrared region. For a given subgraph let l = number of loops, N = number of external lines, V^3 = number of 3-point vertices and V^4 = number of 4-point vertices. Then

$$l=\tfrac{1}{2}V^3+V^4-\tfrac{1}{2}(N-2) \tag{A1}$$

and, in addition, the order of the graph in g is $g^{2l}\times$[order in g of Born graph]. Now let $\dim V_i$ be the dimension of the ith vertex and $\dim P_j$ be the dimension of the jth propagator. Then d is given by

$$d=3l+\sum_{\substack{i\\ \text{vertices}}}\dim V_i+\sum_{\substack{i\\ \text{propagators}}}\dim P_i\,. \tag{A2}$$

Rewriting d as a sum over vertices only is very useful below. First $3l=3+\frac{3}{2}V^3+3V^4-\frac{3}{2}N$ can be rewritten as

TABLE III. d_i for vertices with internal momentum only (see Appendix A).

Vertex	$\frac{3}{2}(n_i-2)$	$\frac{3}{2}l_i$	$\dim V_i$	$\frac{1}{2}\sum_i \dim P_{ij}$	d_i
	$\frac{1}{2}$	0	1	$\frac{1}{2}(-3)$	1
	$\frac{3}{2}$	0	1	$\frac{1}{2}(-5)$	0
	$\frac{3}{2}$	0	0	$\frac{1}{2}(-2)$	$\frac{1}{2}$
	$\frac{3}{2}$	0	0	$\frac{1}{2}(-2)$	$\frac{1}{2}$
	$\frac{3}{2}$	0	1	0	$\frac{3}{2}$
	3	0	0	$\frac{1}{2}(-3)$	1

$$3l = 3 + \sum_{\substack{i \\ \text{vertices}}} \left[\tfrac{3}{2}(n_i - 2) - \tfrac{3}{2}e_i\right], \tag{A3}$$

where n_i = number of lines at vertex i and l_i = number of external particles at vertex i. Since each propagator appears at two vertices,

$$\sum_{\substack{i \\ \text{propagators}}} \dim P_i = \tfrac{1}{2} \sum_{\substack{i \\ \text{vertices}}} \sum_{\substack{j \\ \text{propagators at } i\text{th vertex}}} \dim P_{ij}, \tag{A4}$$

where $\dim P_{ij}$ is the dimension of the jth propagator at the ith vertex. Using Eqs. (A2) and (A4) in Eq. (A3) produces

$$d = 3 + \sum_{\substack{\text{all} \\ \text{vertices}}} \left[\tfrac{3}{2}(n_i - 2) - \tfrac{3}{2}e_i + \dim V_i + \sum_j \dim P_{ij}\right] \tag{A5}$$

Finally define for the ith vertex $d_i \equiv \frac{3}{2}(n_i - 2) - \frac{3}{2}e_i + \dim V_i + \sum_j \dim P_{ij}$. Now consider vertices which contain only internal or loop momenta. The calculation of d_i for each type of vertex is given in Table III. In all cases, $d_i > 0$ and this type of vertex can be ignored in finding the minimum value of d for a type of subgraph. Therefore,

TABLE IV. d_i for vertices with some external momenta (arrows indicate a link with external momenta) (see Appendix A).

	Vertex	$\frac{3}{2}(n_i-2)$	$\dim V_i$	$\frac{1}{2}\sum_j \dim P_{ij}$	d_i
(a)		$\frac{3}{2}$	0	$\frac{1}{2}(-1)$	$1-\frac{3}{2}e_i$
(b)		$\frac{3}{2}$	1	$\frac{1}{2}(-2)$	$\frac{3}{2}-\frac{3}{2}e_i$
(c)		$\frac{3}{2}$	0	$\frac{1}{2}(-1)$	$1-\frac{3}{2}e_i$
(d)		$\frac{3}{2}$	0	$\frac{1}{2}(-1)$	$1-\frac{3}{2}e_i$
(e)		$\frac{3}{2}$	0	$\frac{1}{2}(1)$	$2-\frac{3}{2}e_i$
(f)		$\frac{3}{2}$	0	$\frac{1}{2}(-2)$	$\frac{1}{2}-\frac{3}{2}e_i$
(g)		$\frac{3}{2}$	0	$\frac{1}{2}(0)$	$\frac{3}{2}-\frac{3}{2}e_i$
(h)		$\frac{3}{2}$	0	$\frac{1}{2}(-2)$	$\frac{1}{2}-\frac{3}{2}e_i$
(i)		$\frac{3}{2}$	0	$\frac{1}{2}(0)$	$\frac{3}{2}-\frac{3}{2}e_i$
(j)		$\frac{3}{2}$	0	$\frac{1}{2}(-1)$	$1-\frac{3}{2}e_i$
(k)		3	0	$\frac{1}{2}(-2)$	$2-\frac{3}{2}e_i$
(l)		3	0	$\frac{1}{2}(-1)$	$\frac{5}{2}-\frac{3}{2}e_i$
(m)	Any 3-point vertex with 3 large momenta	$\frac{3}{2}$	0	0	$\frac{3}{2}-\frac{3}{2}e_i$
(n)	4-point vertex with 4 large momenta	3	0	0	$3-\frac{3}{2}e_i$

$$d \geq 3 + \sum_{\substack{i \\ \text{vertices} \\ \text{containing external momentum}}} d_i \tag{A6}$$

and equality is obtained only when all omitted vertices are Coulomb-Coulomb-gluon vertices. Next

d_i must be calculated for vertices carrying external momentum. Here these external momenta are considered as fixed and nonzero. If q_i occurs as an external momenta or combination of momenta, such a subgraph will be treated separately below. The various possible values of d_i are given in Table IV with the fixed momenta indicated by arrows. For $e_i=0$, $d_i \geq \frac{1}{2}$ so that only $e_i>0$ vertices present convergence problems. Vertices containing external lines are classified in a convenient form in Table V. l_i is the number of large (or external) momenta. For a type-one vertex, $d_i=-1$ only for vertices of type (f) and (h) in Table IV.

In case 1, no subset of the external momenta is zero except $\sum_{i=1}^{N} P_i=0$ where P_i is the ith external momentum. Therefore, $P_N=-(P_1+\cdots+P_{N-1})$ and there must be vertices in the graph which link various external momenta to produce P_N. In fact there must be $N-2$ such linkages (a 4-point vertex where three momenta join counts as a two-link vertex and all other relevant vertices are one-link vertices). These linkages must occur at either internal vertices, $e_i=0$, or vertices with external lines, $e_i>0$, and it is possible to find the maximum number of possible links in a given subgraph at vertices with $e_i>0$ by assuming in Table V that the maximum number of linearly independent momenta appear at each vertex. Now define m by $m \equiv$ number of external lines minus the maximum number of links possible in $e_i>0$ vertices, or

$$m=\sum_{e_i>0}[e_i+(1-\text{maximum number of linearly independent large momenta at vertex } i)] \tag{A7a}$$

$$=a_1+b_1-b_4+b_5+b_6\,. \tag{A7b}$$

From the definition of m it is clear that $m-2=$ minimum number of links in $e_i=0$ (internal) vertices. Let

$n_1=$ number of 3-point $e_i=0$ vertices with $l_i=3$,

$n_2=$ number of 4-point $e_i=0$ vertices with $l_i=3$,

$n_3=$ number of 4-point $e_i=0$ vertices with $l_i=4$.

Therefore $n_1+n_2+2n_3 \geq m-2$. However dim (vertex of type n_1) $=\frac{3}{2}$, dim (vertex of type n_2) $=\frac{5}{2}$, dim (vertex of type n_3) $=3$. Therefore

$$\sum_{e_i=0} d_i \geq \tfrac{3}{2}(n_1+\tfrac{5}{3}n_2+2n_3) \geq \tfrac{3}{2}(n_1+n_2+2n_3) \geq \tfrac{3}{2}(m-2)\theta(m-2) \tag{A8}$$

and the θ function can clearly be inserted since $m-2 \geq 0$. Therefore, using Eqs. (A6) and (A8) produces

$$d \geq 3+\tfrac{3}{2}(m-2)\theta(m-2)+\sum_{e_i>0} d_i = 3+\tfrac{3}{2}(m-2)\theta(m-2)-a_1+\tfrac{1}{2}b_1+b_2+\tfrac{3}{2}b_3+\tfrac{3}{2}b_4-\tfrac{1}{2}b_5 \tag{A9}$$

and from Eq. (A7b) comes the final result,

TABLE V. Classification of vertices with external lines (see Appendix A).

Type	e_i	n_i	l_i	Number of linearly independent l_i	Number in subgraph	Do large and small momenta couple?	d_i
(1)	1	3	2	1	a_1	yes	≥ -1
(2)	1	3	3	1 or 2	a_2	no	0
(3)	1	4	2	1	b_1	yes	$\frac{1}{2}$
(4)	1	4	3	1 or 2	b_2	yes	1
(5)	1	4	4	2	b_3	no	$\frac{3}{2}$
(6)	1	4	4	3	b_4	no	$\frac{3}{2}$
(7)	2	4	3	1 or 2	b_5	yes	$-\frac{1}{2}$
(8)	2	4	4	2	b_6	no	0
(9)	2	4	4	3	b_7	no	0

$$d \geq \begin{cases} m > 2 \\ \frac{1}{2}a_1 + 2b_1 + \frac{3}{2}b_2 + \frac{3}{2}b_3 + b_5 + \frac{3}{2}b_6 , \quad m > 2 \text{ or } a_1 + b_1 - b_4 + b_5 + b_6 > 2 \\ \\ m \leq 2 \\ 3 - a_1 + \frac{1}{2}b_1 + b_2 + \frac{3}{2}b_3 + \frac{3}{2}b_4 - \frac{1}{2}b_5 , \quad m \leq 2 \text{ or } a_1 + b_1 - b_4 + b_5 + b_6 \leq 2 . \end{cases} \tag{A10}$$

Inspection of this inequality gives

$$\text{minimum } (d) = 1 \tag{A11a}$$

when

$$a_1 = 2 ,$$
$$b_1 = b_2 = b_3 = b_4 = b_5 = b_6 = 0 ,$$
$$a_2, b_7 \text{ arbitrary}, \tag{A11b}$$

and case (1) is proven since $d \geq 1$.

In case (2) some subset of the external momenta sums to $q \to 0$. In terms of the analysis of case (1), one large-momentum propagator now has small momentum and the most divergent case is for a Coulomb propagator for which $\Delta d = -2$ and $d \geq -1$. To obtain this result more clearly divide the large momenta into two subsets such that in each no partial sum of momenta equals q except the sum of all momenta in the subset. If momenta from the two sets appear at the same vertex then the subgraph is more convergent than in the case of no such vertices. Therefore, to find the minimum value of d, each subset may be considered separately and analyzed as in case (1) so that the minimum value of d is $\min(d) = -1$, when $a_1 = 4$, $b_1 = b_2 = b_3 = b_4 = b_5 = b_6 = 0$, a_2 and b_7 arbitrary. Except for the four a_1-type vertices in this most divergence example of case (2), no vertex couples external momenta to loop momenta since $b_1 = b_2 = b_5 = 0$ (see Table V). Furthermore, to get $d_i = -1$ for an a_1-type vertex the vertex must be of type (f) or (h) in Table IV with the Coulomb line carrying small momentum. The general structure of this type of subgraph is shown in Fig. 10 where $\sum_1^{n_1} P_i = \sum_1^{n_2} Q_i = q \to 0$ and the heavy lines each are $A - E$ or fermion propagators, F contains only loop momenta, G and G' only external momenta and in the most divergent subgraph F contains only Coulomb-Coulomb-gluon vertices. Therefore the dominant infrared structure arises from the longitudinal part of the Hamiltonian. Assume that the subgraph in Fig. 10 gives $d = -1$ so that it behaves as $1/|q|$ as $q \to 0$. Now consider the coefficient of this subgraph. Either G or G' must couple to the distinguished vertex and the part of the graph coupling to this vertex then has the form shown in Fig. 11. G'' contains only large momenta and in it l may be set to zero. The general form of this subgraph is $\overline{D}(q) = \overline{D}^i(q) q_i$, where

$$\overline{D}^i(q) = q^i f_1 + l^i f_2 + \sum_{a=1}^{n_1} P_a^i \alpha^a f_3 ,$$

the f_i being scalar functions of large momenta only and the α_a constants. The q term implies that the entire subgraph acts like $q^i/|q|$ or $d > 0$. The l^i term must have zero coefficient since in $G'' l = 0$

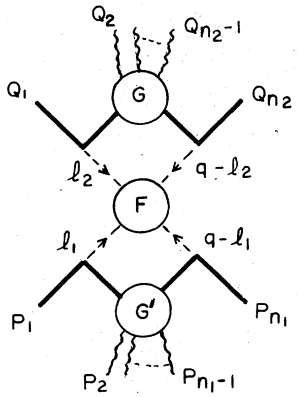

FIG. 10. Most divergent type of subgraph in case (2) (see Appendix A).

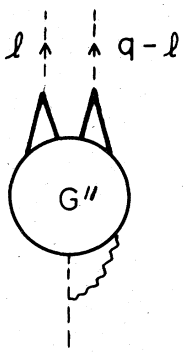

FIG. 11. Coefficient of leading divergence in case 2 (see Appendix A).

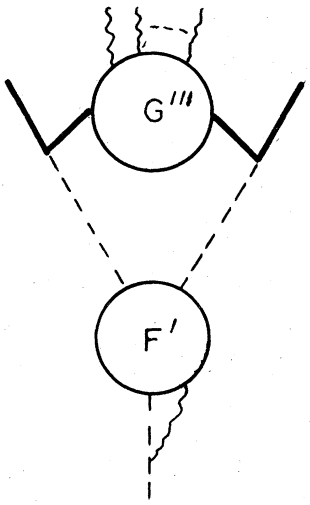

FIG. 12. Most divergent type of graph in case (3) (see Appendix A).

and the two explicit vertices in the graph in Fig. 11 with momentum l in them are either $\vec{A}$-$\vec{E}$-Coulomb or fermion-fermion-Coulomb with the Coulomb line carrying the momentum l, neither of which have a l^i factor. Of course an l_i can appear if the (neglected) l dependence in the propagators is used; e.g.,

$$\frac{1}{|\vec{P}+\vec{l}|}=\frac{1}{P}+\frac{\vec{P}\cdot\vec{l}}{P^3}$$

but then this additional numerator factor of $\vec{P}\cdot\vec{l}$ will make the subgraph in Fig. 10 one less power divergent or $d\geq 0$. Finally consider the $\sum_a P_a^i \alpha^a f_3$ term. f_3 is a scalar function of the P_i and is therefore even under the operation $P_i \to -P_i$. Therefore adding to the subgraphs in Figs. 10 and 11 the contributions with $P_i \to -P_i$ (since the P_i are integration variables in the whole graph) gives zero for this term. Thus in case (2), $d>0$.

Case (3) is now easy. Here all the external momenta except at the distinguished vertex sum to give q. The analysis in case (1) applied to these momenta gives $d>1$. In the most divergent possible case the Coulomb and gluon lines at the distinguished vertex carry only small momentum and analysis as in case (2) gives the form in Fig. 12 as the form of the most divergent type of subgraph with F' similar to F in Fig. 10. The Coulomb line at the distinguished vertex gives $d=-1$ and the gluon line at term $d=-\frac{1}{2}$. However, in F' the minimal value for $d(=1)$ is obtained only when all vertices are Coulomb-Coulomb-gluon vertices. The presence of the gluon line from the distinguished vertex makes it impossible to have all minimal vertices and therefore there is at least one nonminimal vertex giving $\Delta d>\frac{1}{2}$. The sum of the d's is $-1-\frac{1}{2}+\frac{1}{2}=-1$ which implies $d>0$ for case (3).

APPENDIX B: DERIVATION OF THE FOLDY-WOUTHUYSEN TRANSFORMED HAMILTONIAN

In this appendix the Foldy-Wouthuysen transformations described in Sec. IV are explicitly calculated. The Hamiltonian is given by Eq. (2.14),

$$H=\int d^3x\left[\tfrac{1}{2}(\vec{E}_a^{\,2}+\vec{B}_a^{\,2})+\psi^\dagger(-i\vec{\alpha}\cdot\vec{\nabla}+\beta m)\psi-g\psi^\dagger\vec{\alpha}t^a\psi\cdot\vec{A}_a\right]$$

$$+\tfrac{1}{2}\int d^3x\,d^3z\,d^3y\,j_a^0(x)\mathfrak{D}_{ac}(x,z)\nabla_z^2\mathfrak{D}_{cb}(z,y)j_b^0(y)\,. \tag{B1}$$

The goal is to eliminate operators which connect upper and lower spinor indices (or positive- and negative-frequency spinors). Such operators are called "odd." The following Dirac matrices are odd operators:

$$\gamma_5,\quad \beta\gamma_5,\quad \alpha^i,\quad \beta\alpha^i. \tag{B2}$$

The remaining independent operators are "even"; that is, they do not connect positive- and negative-frequency components:

$$1,\quad \beta,\quad \beta\alpha^i\gamma_5,\quad \sigma^{ij}. \tag{B3}$$

For purposes of calculation it is convenient to rewrite Eq. (A1) in the following form:

$$H=\int d^3x\left\{\psi^\dagger(x)[\beta m+\mathcal{O}]\psi(x)+\tfrac{1}{2}(\vec{E}_a^{\,2}+\vec{B}_a^{\,2})+\tfrac{1}{2}j_a^0A_0^a(x)\right\} \tag{B4}$$

where $\mathcal{O}=\vec{\alpha}\cdot\vec{D}$ ($\vec{D}\equiv-i\vec{\nabla}-gt^a\vec{A}^a$) is an odd operator. j_a^0 contains only even terms as does the mass term. The transformation of the Hamiltonian is expressed in terms of a Hermitian operator S such that

$$H' = e^{iS} H e^{-iS} \tag{B5}$$

contains odd operators only in order $1/m$. S itself should be of order $1/m$ so that equation (B5) has the following expansion in $1/m$:

$$H' = H + i[S,H] - \tfrac{1}{2}[S,[S,H]] - \tfrac{i}{6}[S,[S,[S,H]]] + \tfrac{1}{24}[S,[S,[S,[S,H]]]] + \cdots . \tag{B6}$$

In the term quartic in S, only the mass term in H need be considered since the four S's produce a factor $1/m^4$ and no terms of order $1/m^4$ are required. Also in order $1/m^3$ the only terms quartic in S needed are kinetic energy terms. Finding H' will complete the first of the Foldy-Wouthuysen transformations. S is determined by the condition that H' does not have any odd terms of order $(m)^0$. Since S is of order $1/m$, the commutator of S with the mass term in H should cancel the odd terms in Eq. (B4). Clearly the S that satisfies this requirement is

$$S = \frac{-i}{2m}\int d^3x\ \psi^\dagger(x)\beta\mathcal{O}\psi(x) . \tag{B7}$$

Using this S it is straightforward to compute the various commutators needed to determine H' in Eq. (B6). For the commutator of S with H, the following terms are needed:

$$i\left[S, \int d^3y\ \psi^\dagger(x)\beta m\psi(x)\right] = -\int d^3x\ \psi^\dagger(x)\mathcal{O}\psi(x) , \tag{B8a}$$

$$i\left[S, \int d^3x\ \psi^\dagger(x)\mathcal{O}\psi(x)\right] = \frac{1}{m}\int d^3x\ \psi^\dagger(x)\beta\mathcal{O}^2\psi(x) , \tag{B8b}$$

$$i\left[S, \tfrac{1}{2}\int d^3x\ \vec{E}_a^{\,2}\right] = \frac{1}{2m}\int d^3x\ \vec{\mathcal{J}}_a\cdot\vec{E}^a , \tag{B8c}$$

$$i\left[S, \tfrac{1}{2}\int d^3x\ \vec{B}_a^{\,2}\right] = 0 , \tag{B8d}$$

$$i\left[S, \tfrac{1}{2}\int d^3x\ j_a^0 A_0^a\right] = \frac{i}{2m}\int d^3x\ \vec{\nabla}\cdot\vec{\mathcal{J}}_a(x)A_0^a(x) , \tag{B8e}$$

where $\vec{\mathcal{J}}^a = \psi^\dagger(x)\beta\vec{\alpha}gt^a\psi(x)$. Note that Eq. (B8b) contains the magnetic dipole term since $\mathcal{O}^2 = (\vec{\alpha}\cdot\vec{D})^2 = \vec{D}^2 - (g/2)\sigma^{ij}F_{ij}^a t^a$. Combining the above results produces

$$i[S,H] = \int d^3x\left[\psi^\dagger(x)\left(\frac{1}{m}\beta\vec{D}^2 - \vec{\alpha}\cdot\vec{D} - \frac{1}{2m}\beta\sigma^{ij}F_{ij}^a gt^a\right)\psi(x) + \frac{1}{2m}\vec{\mathcal{J}}_a\cdot\vec{E}^a - \frac{1}{2mi}\vec{\nabla}\cdot\vec{\mathcal{J}}_a A_0^a\right] . \tag{B9}$$

Next, using Eq. (A9) the various terms in the double commutator of S with H are found:

$$i\left[S, \frac{1}{m}\int d^3x\ \psi^\dagger\beta\vec{D}^2\psi\right] = -\frac{1}{m^2}\int d^3x\ \psi^\dagger(x)[\tfrac{1}{2}\mathcal{O}\vec{D}^2 + \tfrac{1}{2}\vec{D}^2\mathcal{O}]\psi(x) , \tag{B10a}$$

$$i\left[S, -\int d^3x\ \psi^\dagger(x)\vec{\alpha}\cdot\vec{D}\psi(x)\right] = -\frac{1}{m}\int d^3x\ \psi^\dagger(x)\beta\mathcal{O}\psi(x) , \tag{B10b}$$

$$\begin{aligned} i\left[S, -\frac{1}{2m}\int d^3x\ \psi^\dagger(x)g\beta\sigma^{ij}F_{ija}t^a\psi(x)\right] &= -\frac{1}{m^2}\int d^3x\ \psi^\dagger(x)[i\gamma_5 g^2\{t^a,t^b\}\vec{A}^a\cdot\vec{B}^b + g^2 f^{bac}t^c\vec{\alpha}\cdot(\vec{A}^a\cdot\vec{B}^b)]\psi(x) \\ &\quad + \frac{1}{m^2}\int d^3x\ \psi^\dagger(x)i\gamma_5 gt^a\vec{B}_a\cdot\vec{\nabla}\psi(x) \\ &\quad + \frac{1}{2m^2}\int d^3x\ \psi^\dagger(x)[-\vec{\alpha}\cdot(\vec{\nabla}\times\vec{B}_a)gt^a + i\gamma_5\vec{\nabla}\cdot\vec{B}_a gt^a]\psi(x) , \end{aligned} \tag{B10c}$$

$$\begin{aligned} i\left[S, -\frac{1}{2mi}\int d^3x\ \vec{\nabla}\cdot\vec{\mathcal{J}}_a A_0^a\right] &= \frac{1}{2m^2}\int d^3x\frac{1}{i}\partial_j\{\psi^\dagger(x)\sigma^{ij}D_i gt^a\psi(x)\}A_0^a(x) \\ &\quad + \frac{1}{4m^2}\int d^3x\frac{1}{i}\vec{\nabla}\cdot\{\psi^\dagger(x)\vec{\alpha}\cdot\vec{A}^b g^2 f_{abc}t^c\vec{\alpha}\psi(x)\}A_0^a(x) \\ &\quad - \frac{1}{4m^2}\int d^3x\,d^3z\ d^3y\ \vec{\nabla}\cdot\vec{\mathcal{J}}^a(x)\mathcal{D}_{0c}(x,z)\vec{\nabla}_z^{\,2}\mathcal{D}_{cb}(z,y)\vec{\nabla}\cdot\vec{\mathcal{J}}^b(y) \\ &\quad + \frac{1}{4m^2}\int d^3x\ \psi^\dagger(x)gt^a\psi(x)\nabla^2 A_0^a(x) , \end{aligned} \tag{B10d}$$

$$i\left[S,\frac{1}{2m}\int d^3x\,\vec{\mathcal{J}}^a\cdot\vec{E}_a\right]=\frac{1}{4m^2}\int d^3x\left(\vec{\mathcal{J}}^a\cdot\vec{\mathcal{J}}_a-\vec{\nabla}\cdot\vec{\mathcal{J}}^a\frac{1}{\nabla^2}\vec{\nabla}\cdot\vec{\mathcal{J}}_a\right)$$

$$-\frac{1}{4m^2}\int d^3x\,\psi^\dagger(x)\left[-i\epsilon^{ijk}\sigma^j\left(\frac{1}{i}\partial^k g t^a+\frac{g^2}{\alpha}\{t^a,t^b\}A^b_k\right)+\tfrac{1}{2}g^2 f_{aeb}\,t^e A^i_b(x)\right]\psi(x)E^i_a(x)\,. \tag{B10e}$$

The sum of these terms yields

$$-[S,[S,H]]=-\frac{1}{2m^2}\int d^3x\,\psi^\dagger(x)[\mathcal{O}\vec{D}^2+\vec{D}^2\mathcal{O}]\psi(x)-\frac{1}{m}\int d^3x\,\psi^\dagger(x)\beta\vec{D}^2\psi(x)$$

$$-\frac{1}{4m^2}\int d^3x\,\psi^\dagger(x)\Big\{i\sigma^{ij}\Big(2gt^aE^a_j\frac{1}{i}\partial^i+\Big(\frac{1}{i}\partial^iE^a_j\Big)gt^a$$

$$+g^2A^b_iE^a_j\{t^b,t^a\}\Big)+\tfrac{1}{2}g^2\vec{A}^b\cdot\vec{E}^a[t^b,t^a]\Big\}\psi(x)$$

$$+\frac{1}{4m^2}\int d^3x\left(\vec{\mathcal{J}}_a\cdot\vec{\mathcal{J}}^a-\vec{\nabla}\cdot\vec{\mathcal{J}}^a\frac{1}{\nabla^2}\vec{\nabla}\cdot\vec{\mathcal{J}}_a\right)+\frac{1}{4m^2}\int d^3x\,\psi^\dagger(x)gt^a\psi(x)\nabla^2A^a_0(x)$$

$$+\frac{1}{2m^2}\int d^3x\frac{1}{i}\partial_j\{\psi^\dagger(x)i\sigma^{ij}D_i gt^a\psi(x)\}A^a_0(x)$$

$$+\frac{1}{4m^2}\int d^3x\frac{1}{i}\vec{\nabla}\cdot\{\psi^\dagger(x)\vec{\alpha}\cdot\vec{A}^b g^2t^cf_{abc}\vec{\alpha}\psi(x)\}A^a_0(x)$$

$$-\frac{1}{4m^2}\int d^3x\,d^3z\,d^3y\,\vec{\nabla}\cdot\vec{\mathcal{J}}^a\mathfrak{D}_{ac}(x,z)\nabla_z{}^2\mathfrak{D}_{cb}(z,y)\vec{\nabla}\cdot\vec{\mathcal{J}}^b(y)$$

$$-\frac{1}{m^2}\int d^3x\,\psi^\dagger(x)[i\gamma_5g^2\{t^a,t^b\}\vec{A}^a\cdot\vec{B}^b+g^2f^{bac}t^c\vec{\alpha}\cdot(\vec{A}^a\times\vec{B}_a)]\psi(x)$$

$$+\frac{2i}{m^2}\int d^3x\,\psi^\dagger(x)i\gamma_5gt^a\vec{B}_a\cdot\vec{\nabla}\psi(x)$$

$$+\frac{i}{m^2}\int d^3x\,\psi^\dagger(x)[-\vec{\alpha}\cdot(\vec{\nabla}\times\vec{B}_a)gt^a+i\gamma_5\vec{\nabla}\cdot\vec{B}_agt^a]\psi(x)\,. \tag{B11}$$

For the triple commutator simplifications occur because to order $1/m^3$ in H' only kinetic energy terms are kept:

$$i\left[S,-\frac{1}{2m^2}\int d^3x\,\psi^\dagger(x)[\mathcal{O}\vec{D}^2+\vec{D}^2\mathcal{O}]\psi(x)\right]=-\frac{1}{m^3}\int d^3x\,\psi^\dagger(x)\beta\vec{D}^4\psi(x)+\text{other terms}\,, \tag{B12a}$$

$$i\left[S,-\frac{1}{2m}\int d^3x\,\psi^\dagger(\beta\vec{D}^2\psi(x)\right]=\frac{1}{m^2}\int d^3x\,\psi^\dagger(x)\tfrac{1}{2}(\mathcal{O}\vec{D}^2+\vec{D}^2\mathcal{O})\psi(x)\,. \tag{B12b}$$

Therefore,

$$-i[S,[S,[S,H]]]=-\frac{1}{2m^2}\int d^3x\,\psi^\dagger(x)(\mathcal{O}\vec{D}^2+\vec{D}^2\mathcal{O})\psi(x)-\frac{1}{m^3}\int d^3x\,\psi^\dagger(x)\beta\mathcal{O}^4\psi(x)\,. \tag{B13}$$

Below it is implicit that $1/m^3$ terms include only kinetic energy corrections and all higher-order terms in $1/m$ are omitted. Finally

$$[S,[S,[S,[S,H]]]]=\frac{1}{m^3}\int d^3x\,\psi^\dagger(x)\beta\mathcal{O}^4\psi(x)\,. \tag{B14}$$

Inserting Eqs. (B9), (B11), (B13), and (B14) into Eq. (B6) produces

$$H' = \int d^3x\,\psi^\dagger(x)\left[m\beta+\frac{1}{2m}\beta\vec{D}^2-\frac{1}{6m^2}(\mathcal{O}\vec{D}^2+\vec{D}^2\mathcal{O})-\frac{1}{8m^3}\beta\mathcal{O}^4\right]\psi(x)+\frac{1}{2}\int d^3x\,[(\vec{E}_a^{\,2}+\vec{B}_a^{\,2})+j_a^0A_0^a]$$

$$+\frac{1}{2m}\int d^3x\,[\vec{g}^a\cdot(\vec{E}_a-\vec{\nabla}A_a^0)+\psi^\dagger(x)\beta\vec{\sigma}gt^a\psi(x)\cdot\vec{B}_a(x)]$$

$$+\frac{1}{8m^2}\int d^3x\left(\vec{J}_a\cdot\vec{g}^a-\vec{\nabla}\cdot\vec{g}_a\frac{1}{\nabla^2}\vec{\nabla}\cdot\vec{g}^a\right)+\frac{1}{8m^2}\int d^3x\,\psi^\dagger(x)gt^a\psi(x)\nabla^2A_a^0(x)$$

$$-\frac{1}{8m^2}\int d^3x\,d^3z\,d^3y\,\vec{\nabla}\cdot\vec{g}^a\mathcal{D}_{ac}(x,z)\vec{\nabla}_z^{\,2}\mathcal{D}_{cb}(z,y)\vec{\nabla}\cdot\vec{g}^b(y)$$

$$+\frac{1}{8m^2}\int d^3x\,\psi^\dagger(x)\left[i\epsilon^{ijk}\sigma_j\left(\frac{1}{i}\partial_k t^a+\frac{g^2}{2}\{t^a,t^b\}A_{kb}\right)+\frac{i}{2}f_{aeb}g^2t^eA^{ib}\right]\psi(x)[E_a^i-\partial^iA_a^0]$$

$$+\frac{1}{8m^2}\int d^3x\,\psi^\dagger(x)\left[i\epsilon^{ijk}gt^a\sigma_i\left(\frac{1}{i}\partial_jE_{ka}\right)\right]\psi(x)$$

$$-\frac{1}{2m^2}\int d^3x\,\psi^\dagger(x)[i\gamma_5g^2\{t^a,t^b\}\vec{A}_a\cdot\vec{B}_b+g^2f^{bac}t^c\vec{\alpha}\cdot(\vec{A}_a\times\vec{B}_b)]\psi(x)+\frac{i}{m^2}\int d^3x\,\psi^\dagger(x)i\gamma_5gt^a\vec{B}_a\cdot\vec{\nabla}\psi(x)$$

$$+\frac{i}{2m^2}\int d^3x\,\psi^\dagger(x)[-\vec{\alpha}\cdot(\vec{\nabla}\times\vec{B}_a)gt^a+i\gamma_5\vec{\nabla}\cdot\vec{B}_agt^a]\psi(x)\,, \tag{B15}$$

where

$$\vec{\sigma}=\begin{pmatrix}\vec{\sigma}_p & 0\\ 0 & \vec{\sigma}_p\end{pmatrix}$$

with $\vec{\sigma}_p$ the Pauli spinors. Equation (B15) is the result of the first Foldy-Wouthuysen transformation. The second transformation will eliminate the odd terms of order $1/m$ in H', which are $(1/2m)\int d^3x\,\vec{g}^a\cdot(\vec{E}^a-\vec{\nabla}A_a^0)$, and the choice of S' is again obvious, being

$$S'=-\frac{1}{4m^2}\int d^3x\,\vec{J}_a\cdot[\vec{E}^a-\vec{\nabla}A_a^0]\,, \tag{B16}$$

where $\vec{J}^a=\psi^\dagger(x)gt^a\vec{\alpha}\psi(x)$. The commutator of S' with the mass term eliminates the odd term of order $1/m$. The commutator of S' with the term of order $(m)^0$ gives odd terms which will be removed by S'' and therefore will be ignored. The remaining commutators are of order $1/m^3$ or higher and may be ignored. The effective H'' we obtain is

$$H''=m\int d^3x\,\psi^\dagger(x)\beta\psi(x)+\int d^3x\,\tfrac{1}{2}[(\vec{E}_a^{\,2}+\vec{B}_a^{\,2})+j_a^0A_0^a]$$

$$+\frac{1}{2m}\int d^3x\,[\psi^\dagger(x)\beta\vec{D}^2\psi(x)+\psi^\dagger(x)\beta\vec{\sigma}gt^a\psi(x)\cdot\vec{B}_a(x)]$$

$$+\frac{1}{8m^2}\int d^3x\left(\vec{J}_a\cdot\vec{g}^a-\vec{\nabla}\cdot\vec{g}^a\frac{1}{\nabla^2}\vec{\nabla}\cdot\vec{J}_a\right)-\frac{1}{6m^2}\int d^3x\,\psi^\dagger(x)(\mathcal{O}\vec{D}^2+\vec{D}^2\mathcal{O})\psi(x)$$

$$-\frac{1}{8m^2}\int d^3x\,d^3z\,d^3y\,\vec{\nabla}\cdot\vec{g}^a\mathcal{D}_{ac}(x,z)\vec{\nabla}_z^{\,2}\mathcal{D}_{cb}(z,y)\vec{\nabla}\cdot\vec{g}^b(y)$$

$$+\frac{1}{8m^2}\int d^3x\,\psi^\dagger(x)\left[i\epsilon^{ijk}\sigma_j\left(\frac{1}{i}\partial_kgt^a+\frac{g^2}{2}\{t^a,t^b\}A_b^k\right)+\frac{i}{2}f_{aeb}t^eg^2A_b^i\right]\psi(x)\left(E_i^a-\frac{1}{i}\partial_iA_a^0\right)$$

$$+\frac{1}{8m^2}\int d^3x\,\psi^\dagger(x)gt^a\psi(x)\nabla^2A_a^0+\frac{1}{8m^2}\int d^3x\,\psi^\dagger(x)\left[i\epsilon^{ijk}gt^a\sigma_i\left(\frac{1}{i}\partial_jE_k^a\right)\right]\psi(x)$$

$$-\frac{1}{2m^2}\int d^3x\,\psi^\dagger(x)[i\gamma_5g^2\{t^a,t^b\}\vec{A}_a\cdot\vec{B}_b+g^2f^{bac}t^c\vec{\alpha}\cdot(\vec{A}^a\times\vec{B}^b)]\psi(x)$$

$$+\frac{i}{m^2}\int d^3x\,\psi^\dagger(x)i\gamma_5gt^a\vec{B}^a\cdot\vec{\nabla}\psi(x)+\frac{i}{2m^2}\int d^3x\,\psi^\dagger(x)[-\vec{\alpha}\cdot(\vec{\nabla}\times\vec{B}_a)gt^a+i\gamma_5\vec{\nabla}\cdot\vec{B}_agt^a]\psi(x)$$

$$+\frac{1}{m^2}(\text{odd terms})-\frac{1}{8m^3}\int d^3x\,\psi^\dagger(x)\beta\vec{D}^4\psi(x)\,. \tag{B17}$$

The final Foldy-Wouthuysen transformation will eliminate the odd terms in H'' of order $1/m^2$. In order to remove these terms it is necessary to isolate the odd parts of H'' in order $1/m^2$. Consider, for example, the term $\int d^3x \vec{\mathcal{J}}_a \cdot \vec{\mathcal{J}}^a$, which has both even and odd parts. The even and odd parts are separated by using the projection operators $\frac{1}{2}(1 \pm \beta)$,

$$\vec{\mathcal{J}}^a \cdot \vec{\mathcal{J}}_a = \tfrac{1}{4}\vec{\mathcal{J}}^a_+ \cdot \vec{\mathcal{J}}_{+a} + \tfrac{1}{2}\vec{\mathcal{J}}^a_+ \cdot \vec{\mathcal{J}}_{-a} + \tfrac{1}{4}\vec{\mathcal{J}}^a_- \cdot \vec{\mathcal{J}}_{-a}, \tag{B18}$$

where $\vec{\mathcal{J}}^a_\pm(x) = \psi^\dagger(x)\beta\vec{\alpha}gt^a(1 \pm \beta)\psi(x)$. The term $\vec{\mathcal{J}}^a_+(x) \cdot \vec{\mathcal{J}}^a_-(x)$ is an even term, as may be shown by using the Fierz reordering theorem

$$\psi_1^\dagger\vec{\alpha}(1+\beta)\psi_2 \cdot \psi_3^\dagger\vec{\alpha}(1-\beta)\psi_4 = \tfrac{3}{2}\psi_1^\dagger(1-\beta)\psi_4\psi_3^\dagger(1+\beta)\psi_2 - \tfrac{1}{2}\psi_1^\dagger\sigma^{ij}(1-\beta)\psi_4\psi_3^\dagger\sigma^{ij}(1+\beta)\psi^2 \tag{B19}$$

(internal degrees of freedom have been suppressed). $\vec{\mathcal{J}}^a_+ \cdot \vec{\mathcal{J}}^a_+$ and $\vec{\mathcal{J}}^a_- \cdot \vec{\mathcal{J}}^a_-$ are odd. Therefore the odd terms of H'' may be isolated as follows:

$$\begin{aligned}
(H''_{\text{odd}})_{1/m^2} = &-\frac{1}{3m^2}\int d^3x\, \psi^\dagger(x)\tfrac{1}{2}(\Theta\vec{D}^2 + \vec{D}^2\Theta)\psi(x) \\
&+\frac{1}{32m^2}\int d^3x\left[\vec{\mathcal{J}}^a_+ \cdot \vec{\mathcal{J}}_{+a} + \vec{\mathcal{J}}^a_- \cdot \vec{\mathcal{J}}_{-a} - \vec{\nabla}\cdot\vec{\mathcal{J}}^a_+\frac{1}{\nabla^2}\vec{\nabla}\cdot\vec{\mathcal{J}}_{+a} - \vec{\nabla}\cdot\vec{\mathcal{J}}^a_-\frac{1}{\nabla^2}\vec{\nabla}\cdot\vec{\mathcal{J}}_{-a}\right] \\
&-\frac{1}{32m^2}\int d^3x\, d^3z\, d^3y\,[\vec{\nabla}\cdot\vec{\mathcal{J}}^a_+\mathfrak{D}_{ac}(x,z)\vec{\nabla}_z^2\mathfrak{D}_{cb}(z,y)\vec{\nabla}\cdot\vec{\mathcal{J}}^b_+(y) + \vec{\nabla}\cdot\vec{\mathcal{J}}^a_-\mathfrak{D}_{ac}(x,z)\vec{\nabla}_z^2\mathfrak{D}_{cb}(z,y)\vec{\nabla}\cdot\vec{\mathcal{J}}^b_-(y)] \\
&-\frac{1}{2m^2}\int d^3x\,\psi^\dagger(x)[i\gamma_5 g^2\{t^a,t^b\}\vec{A}^a\cdot\vec{B}^b + g^2 f^{bac}t^c\vec{\alpha}\cdot(\vec{A}^a\times\vec{B}^b)]\psi(x) + \frac{i}{m^2}\int d^3x\,\psi^\dagger(x)i\gamma_5 gt^a\vec{B}_a\cdot\vec{\nabla}\psi(x) \\
&+\frac{i}{2m^2}\int d^3x\,\psi^\dagger(x)[-\vec{\alpha}\cdot(\vec{\nabla}\times\vec{B}_a)gt^a + i\gamma_5\vec{\nabla}\cdot\vec{B}_a gt^a]\psi(x) - \frac{i}{4m^2}\left[S', \int d^3x\,\tfrac{1}{2}[(\vec{E}_a^{\,2} + \vec{B}_a^{\,2}) + j^0_a A^a_0]\right].
\end{aligned} \tag{B20}$$

The only complication in finding an S'' to eliminate the right-hand side of Eq. (B20) is in some of the terms quartic in the fermion fields. For terms quadratic in the fermion fields and for quartic terms with only one $\vec{\alpha}$ matrix, the correct form for S'' is obtained by inserting the Dirac matrix β between the fermion-antifermion pairs which contain an $\vec{\alpha}$. The quartic terms with more than one $\vec{\alpha}$ are of the form $\vec{\mathcal{J}}^a_+ \cdot \vec{\mathcal{J}}^a_+$, where the projection matrixes make the placement of the additional β irrelevant. Therefore S'' may be constructed. The final form of the Hamiltonian is

$$\begin{aligned}
H''' = &\, m\int d^3x\,\psi^\dagger(x)\beta\psi(x) + \tfrac{1}{2}\int d^3x\,[(\vec{E}_a^{\,2} + \vec{B}_a^{\,2}) + j^0_a A^a_0] \\
&+\frac{1}{2m}\int d^3x\,[\psi^\dagger(x)\beta\vec{D}^2\psi(x) + \psi^\dagger(x)\beta\vec{\sigma}gt^a\psi(x)\cdot\vec{B}_a(x)] \\
&+\frac{1}{16m^2}\int d^3x\left[\vec{\mathcal{J}}^a_+\cdot\vec{\mathcal{J}}_{-a} - \vec{\nabla}\cdot\vec{\mathcal{J}}^a_+\frac{1}{\nabla^2}\vec{\nabla}\cdot\vec{\mathcal{J}}_{-a}\right] + \frac{1}{8m^2}\int d^3x\,\psi^\dagger(x)gt^a\psi(x)\nabla^2 A^a_0(x) \\
&-\frac{1}{16m^2}\int d^3x\, d^3z\, d^3y\;\vec{\nabla}\cdot\vec{\mathcal{J}}^a_+\mathfrak{D}_{ac}(x,z)\vec{\nabla}_z^2\mathfrak{D}_{cb}(z,y)\vec{\nabla}\cdot\vec{\mathcal{J}}^b_-(y) \\
&+\frac{1}{8m^2}\int d^3x\,\psi^\dagger(x)\left[i\epsilon^{ijk}\sigma_j\left(\frac{1}{i}\partial_k gt^a + \frac{g^2}{2}\{t^a,t^b\}A^k_b\right) + \frac{i}{2}f_{aeb}g^2t^eA^i_b\right]\psi(x)\left[E^i_a - \frac{1}{i}\partial^i A^0_a\right] \\
&+\frac{1}{8m^2}\int d^3x\,\psi^\dagger(x)\,i\epsilon^{ijk}gt^a\sigma_i\left(\frac{1}{i}\partial_j E^a_k\right)\psi(x) - \frac{1}{8m^3}\int d^3x\,\psi^\dagger(x)\beta\vec{D}^4\psi(x)\quad .
\end{aligned} \tag{B21}$$

APPENDIX C: PERTURBATION THEORY CALCULATIONS

In this appendix the explicit calculations are given for the one-loop kernel and for graph (a) in Table II, which contributes to the two-loop kernel, by means of dimensional regulations. The one-loop graph in Fig. 6(a) may be written analytically as

$$i\bar{u}(p,\lambda_1)\gamma^0 u(p_1'\lambda_1')\bar{v}(p_1'\lambda_2)\gamma^0 v(p_1\lambda_2')\sum_\alpha t_{ij}^\alpha t_{kl}^\alpha \frac{g^2}{\vec{q}^2}\mathcal{J}_2(q^2;n)C_2$$

where $n-1$ = the number of space dimensions and

$$\begin{aligned}\mathcal{J}_2(q^2,n) &= -3g^2\frac{1}{q^2}\int\frac{d^{n-1}k}{(2\pi)^3}q_i q_j\left(\delta_{ij}-\frac{k_i k_j}{k^2}\right)\frac{1}{2k}\frac{1}{(\vec{q}-\vec{k})^2}\\ &= \frac{-3g^2}{16\pi^3}\int_0^\infty dx\, x^{n-3}\int d\Omega^{n-1}\frac{1-\cos^2\theta}{1+x^2-2x\cos\theta}q^{n-4}\\ &= -\frac{3g^2}{16\pi^3}\int_0^\infty dx\, x^{n-3}q^{n-4}2\pi\left\{\frac{1+x^2}{2x^2}+\frac{1}{x}\frac{(1-x)^2}{4x^2}\ln\left|\frac{1-x}{1+x}\right|\right\}\\ &= -\frac{3g^2}{16\pi^2}(q^2)\frac{n-4}{2}\int_0^\infty dx\, x^{n-3-2}\left\{1+x^2+\frac{(1-x^2)}{2x}\ln\left|\frac{1-x}{1+x}\right|\right\}.\end{aligned} \tag{C1}$$

As $n\to 4$,

$$(q^2)\frac{n-4}{2}=\exp\left\{(\ln q^2)\frac{n-4}{2}\right\}=1+(\ln q^2)\left(\frac{n-4}{2}\right)+\tfrac{1}{2}(\ln q^2)^2\left(\frac{n-4}{2}\right)^2+\cdots, \tag{C2}$$

$$\begin{aligned}\int_0^\infty dx\, x^{n-5}\left\{1+x^2+\left(\frac{(1-x^2)^2}{2x}\ln\left|\frac{1-x}{1+x}\right|\right)\right\} &= \int_1^\infty dx\, x^{n-5}\left\{1+x^2+\frac{(1-x^2)^2}{2x}(-2)\left(\frac{1}{x}+\frac{1}{3x^3}\right)+\cdots\right.\\ &\quad\left.+\int_0^1 dx\, x^{n-5}\left\{1+x^2+\frac{(1-x^2)^2}{2x}\ln\frac{1-x}{1+x}\right\}\right.\end{aligned} \tag{C3a}$$

$$\xrightarrow[n\to 4]{}\int_1^\infty dx\, x^{n-5}\left\{1+x^2-\frac{x^4-2x^2+1}{x^2}\left(1+\frac{1}{3x^2}\right)\right\}+\text{Reg}=\frac{8}{3}\frac{1}{n-4}+\text{Reg}. \tag{C3b}$$

Therefore $\mathcal{J}_2(q^2,n)$ becomes as $n\to 4$,

$$\mathcal{J}_2(q^2,n)=-\frac{3g^2}{16\pi^2}\left[1+(\ln q^2)\frac{n-4}{2}+\tfrac{1}{2}(\ln q^2)^2\left(\frac{n-4}{2}\right)^2\right]\left[\frac{8}{3}\frac{1}{n-4}+\text{Reg}\right] \tag{C4}$$

and subtracting the integral at the renormalization point μ gives

$$\mathcal{J}_2(q^2,n)-\mathcal{J}_2(\mu^2,n)=-\frac{3g^2}{16\pi^2}\left[\frac{1}{2}\left(\ln\frac{q^2}{\mu^2}\right)\frac{8}{3}\right]+\text{Reg} \tag{C5}$$

so that $[\mathcal{J}_2(q^2)\equiv\mathcal{J}_2(q^2,4)]$

$$\mathcal{J}_2(q^2)-\mathcal{J}_2(\mu^2)=-\frac{g^2}{4\pi^2}\ln\frac{q^2}{\mu^2}. \tag{C6}$$

For the other one-loop contribution to the kernel, Fig. 6(b), the analytic expression is (using the same notation as above)

$$i\bar{u}(p_1\lambda_1)\gamma^0 u(p_1'\lambda_1')\bar{v}(p_1'\lambda_2')\gamma^0 v(p_1'\lambda_2)\sum_\alpha t_{ij}^\alpha t_{kl}^\alpha\frac{g^2}{q^2}\mathcal{J}_1(q^2,n)C_2,$$

where

$$\mathcal{J}_1(q^2,n)=\frac{g^2}{q^2}\int\frac{d^{n-1}k}{(2\pi)^3}\frac{1}{2k}\frac{1}{2|\vec{q}-\vec{k}|}\frac{2}{k+|\vec{q}-\vec{k}|}\left(\delta_{ij}-\frac{k_ik_j}{k^2}\right)\left(\delta_{ji}-\frac{(q-k)_j(q-k)_i}{(q-k)^2}\right)k(k-|\vec{q}-\vec{k}|)$$

$$=\frac{g^2}{16\pi^3}\frac{1}{q^2}\int d^{n-1}k\frac{|\vec{k}-\vec{q}/2|-|\vec{k}+\vec{q}/2|}{|\vec{k}-\vec{q}/2|+|\vec{k}+\vec{q}/2|}\left[(k^2+q^2/4)^2-(\vec{k}\cdot\vec{q})^2+(k^2-q^2/4)^2\right]$$

$$\times\frac{1}{|\vec{k}+\vec{q}/2|}\frac{1}{(k^2+q^2/4)^2-(\vec{q}\cdot\vec{k})^2}\qquad(\vec{q}\cdot\vec{k}=qk\alpha)$$

$$=-\frac{g^2}{16\pi^3}\int_0^\infty dx\int d\Omega_{n-1}x^{n-2}q^{n-4}\frac{(\frac{1}{4}+x^2+\alpha x)^{1/2}-(\frac{1}{4}+x^2-\alpha x)^{1/2}}{(\frac{1}{4}+x^2+\alpha x)^{1/2}+(\frac{1}{4}+x^2-\alpha x)^{1/2}}$$

$$\times\left[(x^2+\tfrac{1}{4})^2-x^2\alpha^2+(x^2-\tfrac{1}{4})^2\right]\frac{1}{(\frac{1}{4}+x^2+\alpha x)^{1/2}}\frac{1}{(x^2+\frac{1}{4})^2-x^2\alpha^2}$$

$$=-\frac{g^2}{2\pi^3}\frac{2\pi^{(n-2)/2}}{\Gamma((n-1)/2)}\int_0^\infty dx\int_{-1}^1 d\alpha\frac{x^{n-2}q^{n-4}}{2^{n-1}}\frac{(1+x^2+2\alpha x)^{1/2}-(1+x^2-2\alpha x)^{1/2}}{(1+x^2+2\alpha x)^{1/2}+(1+x^2-2\alpha x)^{1/2}}$$

$$\times\left[\tfrac{1}{2}x^4+\tfrac{1}{2}-\alpha^2x^2\right]\frac{1}{(1+x^2+2\alpha x)^{1/2}}\frac{1}{(1+x^2)^2-4x^2\alpha^2},\qquad\xi=\frac{x^2+1}{x}$$

$$=-\frac{g^2}{\pi^3}\frac{\pi^{(n-2)/2}}{\Gamma((n-2)/2)}\frac{1}{2^{n-3}}\int_0^\infty dx\int_{-1}^1 d\alpha\,x^{n-5/2}\frac{\alpha}{\xi+(\xi^2-4\alpha^2)^{1/2}}(\xi^2-2-2\alpha^2)\frac{1}{\xi^2-4\alpha^2}\frac{1}{(\xi+2\alpha)^{1/2}}q^{n-4},\qquad\text{(C7a)}$$

$$\xrightarrow[n-4]{}-\frac{g^2}{8\pi^2}\int_1^\infty dx\int_{-1}^1 d\alpha\,x^{n-5/2}\left[\frac{\alpha}{2x}\left(1+\frac{\alpha^2}{x}\right)(x^2-2\alpha^2)\frac{1}{x^2}\left(1+\frac{4\alpha^2-1}{x^2}\right)\frac{1}{\sqrt{x}}\left(1-\frac{\alpha}{x}\right)\right.$$

$$\left.+\text{higher-order }\frac{1}{x}\text{ terms}\right]\left[1+(\ln q^2)\frac{n-4}{2}+\cdots\right]$$

$$=-\frac{g^2}{8\pi^2}\int_1^\infty dx\int_{-1}^1 d\alpha\left[\left(-\frac{\alpha^2}{2}\right)x^{n-5}+O(x^{n-6})\right]\left[1+(\ln q^2)\frac{n-4}{2}+\cdots\right]$$

$$=-\frac{g^2}{8\pi^2}\left(-\frac{1}{3}\frac{1}{n-4}+\text{Reg}\right)\left[1+(\ln q^2)\frac{n-4}{2}+\cdots\right].\qquad\text{(C7b)}$$

Therefore,

$$\mathcal{J}_1(q^2,n)-\mathcal{J}_1(\mu^2,n)=-\frac{g^2}{8\pi^2}\left(-\frac{1}{3}\frac{1}{n-4}+\text{Reg}\right)\left(\ln\frac{q^2}{\mu^2}\right)\frac{n-4}{2}\qquad\text{(C8)}$$

and

$$\mathcal{J}_1(q^2)-\mathcal{J}_1(\mu^2)=\frac{g^2}{48\pi^2}\ln\frac{g^2}{\mu^2}.\qquad\text{(C9)}$$

The sum of Eqs. (C6) and (C9) with the appropriate kinematic and group factors produces the one-loop kernel K_1 (for the singlet state),

$$K_1=\frac{ig^2}{q^2}C_2T_2N\left(-\frac{g^2}{4\pi^2}\ln\frac{q^2}{\mu^2}+\frac{g^2}{48\pi^2}\ln\frac{q^2}{\mu^2}\right)\qquad\text{(C10a)}$$

$$=\frac{ig^2}{q^2}T_2N\left[-g^2C_2\frac{11}{3}\frac{1}{16\pi^2}\ln\frac{q^2}{\mu^2}\right].\qquad\text{(C10b)}$$

The final calculation in the appendix is for graph (a) in Table II, which is given by (for the singlet state)

$$\frac{ig^6}{q^2}\int\frac{d^3l}{(2\pi)^3}\frac{d^3k}{(2\pi)^3}\,\text{Tr}\left[t^at^bt^at^b\right]C_2\left(\frac{-i}{l^2}\right)^2\left[\delta_{ij}-\frac{k_ik_j}{k^2}\right]$$

$$\times\left[\delta_{ij}-\frac{(k_i-l_i)(k_j-l_j)}{(k-l)^2}\right]\frac{1}{2k}\frac{i}{2|\vec{k}-\vec{l}|}((\vec{l}-\vec{k})^2-|\vec{l}-\vec{k}|k)\frac{-i}{\epsilon_1-|\vec{k}|-|\vec{k}-\vec{l}|}\frac{-i}{\epsilon_2-k-|\vec{k}-\vec{l}|}$$

$$=\frac{ig^6}{q^2}C_2T_2N(T_2-\tfrac{1}{2}C_2)I,\qquad\text{(C11a)}$$

where

$$I=\int\frac{d^3l}{(2\pi)^3}\frac{d^3k}{(2\pi)^3}\frac{1}{l^4}\frac{1}{4k}(|\vec{l}-\vec{k}|-k)\left(1+\frac{[\vec{k}\cdot(\vec{k}-\vec{l})]^2}{k^2(\vec{l}-\vec{k})^2}\right)\frac{1}{k+|\vec{l}-\vec{k}|-\epsilon_1}\frac{1}{k+|\vec{l}-\vec{k}|-\epsilon_2}$$

$$=\int\frac{d^3l}{(2\pi)^3}\frac{d^3k}{(2\pi)^3}\int_0^\infty d\alpha\int_0^\infty d\beta\,\delta(\alpha-k)\delta(|\vec{l}-\vec{k}|-\beta)\frac{1}{l^4}\frac{1}{4k}(|\vec{l}-\vec{k}|-k)$$

$$\times\left(1+\frac{[\frac{1}{2}k^2+\frac{1}{2}l^2+\frac{1}{2}(\vec{k}-\vec{l})^2]}{k^2(l-k)^2}\right)\frac{1}{k+|\vec{l}-\vec{k}|-\epsilon_1}\frac{1}{k+|\vec{l}-\vec{k}|-\epsilon_2}$$

$$=\int_0^\infty l^2dl\frac{2}{(2\pi)^2}\int_0^\infty d\alpha\int_0^\infty d\beta\frac{\alpha}{(2\pi)^2}\frac{\beta}{\alpha}\theta(\alpha+l-\beta)\theta(\beta-|\alpha-l|)\frac{1}{l^4}\frac{1}{4\alpha}(\beta-\alpha)$$

$$\times\left(1+\frac{[\frac{1}{2}\alpha^2+\frac{1}{2}\beta^2-\frac{1}{2}l^2]^2}{\alpha^2\beta^2}\right)\frac{1}{\alpha+\beta-\epsilon_1}\frac{1}{\alpha+\beta-\epsilon_2}$$

$$=\frac{1}{2(2\pi)^4}\int_0^\infty\frac{dl}{l^3}\int_0^\infty d\alpha\int_{|\alpha-l|}^{|\alpha+l|}d\beta(\beta^2-\alpha\beta)\left[1+\frac{(\alpha^2+\beta^2-l^2)^2}{4}\right]\frac{1}{\alpha+\beta-t_1}\frac{1}{\alpha+\beta-\epsilon_2}$$

$$=\frac{1}{2(2\pi)^4}\int_0^\infty\frac{dl}{l}\int_0^\infty d\alpha\int_{|\alpha-1|}^{|\alpha+1|}d\beta(\beta^2-\alpha\beta)\left[1+\frac{(\alpha^2+\beta^2-1)^2}{4\alpha^2\beta^2}\right]\frac{1}{\alpha+\beta-\epsilon_1/l}\frac{1}{\alpha+\beta-\epsilon_2/l},\quad(\eta=\alpha+\beta;\ \chi=\alpha-\beta)$$

$$=\frac{1}{8(2\pi)^4}\int_0^\infty\frac{dl}{l}\int_1^\infty d\eta\frac{1}{\eta-\epsilon_1/l}\frac{1}{\eta-\epsilon_2/l}\int_{-1}^1 d\chi\,\chi^2\left[1+\frac{(\eta^2+\chi^2-2)^2}{(\eta^2-\chi^2)^2}\right].\tag{C12}$$

It can be shown by elementary methods that

$$\int_{-1}^1 d\chi\,\chi^2\frac{(2-\eta^2-\chi^2)}{(\chi^2-\eta^2)^2}=\tfrac{4}{3}+12(\eta^2-1)+2(3\eta^2-1)\frac{1-\eta^2}{\eta}\ln\frac{\eta+1}{\eta-1},\tag{C13}$$

so that

$$I=\frac{1}{8(2\pi)^4}\int_1^\infty\frac{d\eta}{\eta^2}\int_0^\infty\frac{l}{(l+\epsilon_1/\eta)(l+\epsilon_2/\eta)}\left[\tfrac{4}{3}+12(\eta^2-1)-2(3\eta^2-1)\frac{\eta^2-1}{\eta}\ln\frac{\eta+1}{\eta-1}\right]\tag{C14}$$

in which $\epsilon_1,\epsilon_2\to|\epsilon_1|,|\epsilon_2|$ with $\epsilon_1,\epsilon_2<0$. The l integration is done by dimensional regularization as follows:

$$\mathcal{I}=\int_0^\infty dl\frac{l}{(l+\epsilon_1/\eta)(l+\epsilon_2/\eta)}\longrightarrow\mathcal{I}_n=\frac{1}{4\pi}\frac{2\pi^{(n-1)/2}}{\Gamma((n-1)/2)}\int_0^\infty dl\,l^{n-3}\frac{\eta}{\epsilon_2-\epsilon_1}\left[\frac{1}{l+\epsilon_1/\eta}-\frac{1}{l+\epsilon_2/\eta}\right],\tag{C15}$$

$$\mathcal{I}_n=\frac{\pi^{(n-3)/2}}{2\Gamma((n-1)/2)}\frac{\eta}{\epsilon_2-\epsilon_1}\left[\left(\frac{\epsilon_1}{\eta}\right)^{n-3}-\left(\frac{\epsilon_2}{\eta}\right)^{n-3}\right]\frac{\Gamma(n-2)}{3-n}\Gamma(4-n)\qquad\left(\int_0^\infty dx\frac{x^{n-3}}{x+a}=a^{n-3}\Gamma(n-2)\Gamma(3-n)\right)\tag{C16a}$$

$$\xrightarrow[n\to4]{}\frac{1}{4-n}+\frac{\epsilon_1\ln\epsilon_1-\epsilon_2\ln\epsilon_2}{\epsilon_2-\epsilon_1}+\text{constants}+\ln\eta+O(n-4)\tag{C16b}$$

$$\equiv A+\ln\eta+O(n-4).\tag{C16c}$$

The integral I now becomes $[\eta\to(1/\eta)]$

$$I=\frac{1}{8(2\pi)^4}\int_0^1 d\eta[A-\ln\eta]\left[\frac{4}{3}-\frac{12}{\eta^2}(1-\eta^2)-\frac{2}{\eta^3}(3-\eta^2)(1-\eta^2)\ln\frac{1+\eta}{1-\eta}\right]\tag{C17a}$$

$$=\frac{1}{8(2\pi)^4}\int_0^1 d\eta[A-\ln\eta]\left[\tfrac{4}{3}-12+\frac{2}{\eta}(4-\eta^2)\ln\frac{1+\eta}{1-\eta}+\frac{12}{\eta^2}-\frac{6}{\eta^3}\ln\frac{1+\eta}{1-\eta}\right].\tag{C17b}$$

To evaluate Eq. (C17b) the following integrals are needed:

$$\int_0^1 d\eta[A-\ln\eta]=A+1\,, \tag{C18a}$$

$$\int_0^1 d\eta[A-\ln\eta]\left[\frac{12}{\eta^2}-\frac{6}{\eta^3}\ln\frac{1+\eta}{1-\eta}\right]=6(\tfrac{1}{2}-A)-6\frac{\pi^2}{8}\,, \tag{C18b}$$

$$\int_0^1 d\eta\,\eta\ln\frac{1+\eta}{1-\eta}=1\,, \tag{C18c}$$

$$\int_0^1 d\eta\frac{1}{\eta}\ln\frac{1+\eta}{1-\eta}=\frac{\pi^2}{4}\,, \tag{C18d}$$

$$\int_0^1 d\eta(\ln\eta)\left(\frac{4}{\eta}-\eta\right)\ln\frac{1+\eta}{1-\eta}=-7\zeta(3)-\frac{\pi^2}{8}+\frac{3}{2}\,. \tag{C18e}$$

ζ is the Riemann zeta function. Plugging Eqs. (C18) into Eq. (C17b) gives

$$I=\frac{1}{8(2\pi)^4}\left[(A+1)(\tfrac{4}{3}-12)-2A+\frac{8\pi^2}{4}A+14\xi(3)+\frac{\pi^2}{4}-3-6(A-\tfrac{1}{2})-6\frac{\pi^2}{8}\right] \tag{C19a}$$

$$=\frac{1}{8(2\pi)^4}\left[\left(\frac{1}{4-n}+\frac{\epsilon_1\ln\epsilon_1-\epsilon_2\ln\epsilon_2}{\epsilon_2-\epsilon_1}+\text{constants}\right)(2\pi^2-\tfrac{56}{3})-\left(\frac{\pi^2}{2}-14\xi(3)+\tfrac{32}{3}\right)\right]\,. \tag{C19b}$$

Subtracting I at $\epsilon_1=\epsilon_2=\lambda$ and setting $n=4$ produces

$$I^R=I-I(\lambda^2)$$

$$=\frac{1}{8(2\pi)^4}(2\pi^2-\tfrac{56}{3})\left(\frac{\epsilon_1\ln(\epsilon_1{}^2/\lambda^2)-\epsilon_2\ln(\epsilon_2{}^2/\lambda^2)}{2(\epsilon_2-\epsilon_1)}+1\right)\,, \tag{C20}$$

which gives the desired result when inserted into Eq. (C11b).

---

[1]A comprehensive review of J/ψ phenomenology may be found in K. Gottfried, Proceedings of the 1977 International Symposium on Lepton and Photon Interactions at High Energies (unpublished); and Cornell Report No. CLNS-376 (unpublished).

[2]F. Feinberg, Phys. Rev. Lett. 39, 316 (1977).

[3]See, for example, H. Bethe and E. Salpeter, *Quantum Mechanics of One- and Two-Electron Atoms* (Springer, Berlin, 1957).

[4]L. Foldy and S. Wouthuysen, Phys. Rev. 78, 29 (1950).

[5]Z. Chraplyvy, Phys. Rev. 91, 388 (1953); 92, 1310 (1953); W. Barker and F. Glover, *ibid.* 99, 317 (1955).

[6]T. Appelquist, M. Dine, and I. J. Muzinich, Phys. Lett. 69B, 231 (1977).

[7]T. Appelquist, M. Dine, and I. J. Muzinich, Phys. Rev. D 17, 2074 (1978).

[8]W. Fischler, Nucl. Phys. B129, 157 (1977); L. Susskind, in Lectures given at the Les Houches School on High Energy Physics, 1976 (unpublished).

[9]E. Poggio, Phys. Rev. D 16, 2605 (1977).

[10]E. Eichten and K. Gottfried, Phys. Lett. 66B, 286 (1977).

[11]J. Schwinger, Phys. Rev. 125, 1043 (1962).

[12]J. Schwinger, Phys. Rev. 127, 324 (1962).

[13]S. Mandelstam, invited talk given at the Washington Meeting of the American Physical Society, 1977 (unpublished).

[14]V. N. Gribov, lecture at the 12th Winter School of the Leningrad Nuclear Physics Institute, 1977, Report No. SLAC-TRANS-176 (unpublished).

[15]J. Schwinger, Phys. Rev. 128, 2425 (1962).

[16]T. Appelquist and J. Carazzone, Phys. Rev. D 11, 2856 (1975).

[17]J. Schwinger, Proc. Natl. Acad. Sci. USA 37, 452 (1951); 37, 455 (1951).

[18]H. Bethe and E. Salpeter, Phys. Rev. 84, 1232 (1951).

[19]E. Salpeter, Phys. Rev. 87, 328 (1952).

[20]S. Mandelstam, Proc. R. Soc. London A233, 248 (1955).

[21]A. Duncan, Phys. Rev. D 10, 2866 (1976); J. Frenkel and J. C. Taylor, Nucl. Phys. B109, 439 (1976); B117, 546(E) (1976).

[22]S. Davis and F. Feinberg (unpublished).

[23]E. Eichten and F. Feinberg (unpublished).

[24]R. Jackiw, I. Muzinich, and C. Rebbi, Phys. Rev. D 17, 1576 (1978).